frontiers | Frontiers in Forests and Global Change

TYPE Original Research
PUBLISHED 12 September 2023
DOI 10.3389/ffgc.2023.1146033

OPEN ACCESS

EDITED BY
John Robert Healey,
Bangor University, United Kingdom

REVIEWED BY
Andrey Krasovskiy,
International Institute for Applied Systems Analysis (IIASA), Austria
Romà Ogaya,
Ecological and Forestry Applications Research Center (CREAF), Spain

*CORRESPONDENCE
Jeffrey E. Stenzel
✉ jeffrey.e.stenzel@gmail.com

RECEIVED 16 January 2023
ACCEPTED 16 August 2023
PUBLISHED 12 September 2023

CITATION
Stenzel JE, Kolden CA, Buotte PC, Bartowitz KJ, Walsh EW and Hudiburg TW (2023) Vulnerability of northern rocky mountain forests under future drought, fire, and harvest.
Front. For. Glob. Change 6:1146033.
doi: 10.3389/ffgc.2023.1146033

Vulnerability of northern rocky mountain forests under future drought, fire, and harvest

Jeffrey E. Stenzel[1]*, Crystal A. Kolden[1], Polly C. Buotte[2], Kristina J. Bartowitz[3,4], Eric W. Walsh[5] and Tara W. Hudiburg[4]

[1]Management of Complex Systems, University of California Merced, Merced, CA, United States, [2]Energy and Resources Group, University of California, Berkeley, Berkeley, CA, United States, [3]American Forests, Washington, DC, United States, [4]Department of Forest, Rangeland, and Fire Sciences, University of Idaho, Moscow, ID, United States, [5]Manomet, Plymouth, MA, United States

Novel climate and disturbance regimes in the 21st century threaten to increase the vulnerability of some western U.S. forests to loss of biomass and function. However, the timing and magnitude of forest vulnerabilities are uncertain and will be highly variable across the complex biophysical landscape of the region. Assessing future forest trajectories and potential management impacts under novel conditions requires place-specific and mechanistic model projections. Stakeholders in the high-carbon density forests of the northern U.S. Rocky Mountains (NRM) currently seek to understand and mitigate climate risks to these diverse conifer forests, which experienced profound 20th century disturbance from the 1910 "Big Burn" and timber harvest. Present forest management plan revisions consider approaches including increases in timber harvest that are intended to shift species compositions and increase forest stress tolerance. We utilize CLM-FATES, a dynamic vegetation model (DVM) coupled to an Earth Systems Model (ESM), to model shifting NRM forest carbon stocks and cover, production, and disturbance through 2100 under unprecedented climate and management. Across all 21st century scenarios, domain forest C-stocks and canopy cover face decline after 2090 due to the interaction of intermittent drought and fire mortality with declining Net Primary Production (NPP) and post-disturbance recovery. However, mid-century increases in forest vulnerability to fire and drought impacts are not consistently projected across climate models due to increases in precipitation that buffer warming impacts. Under all climate scenarios, increased harvest regimes diminish forest carbon stocks and increase period mortality over business-as-usual, despite some late-century reductions in forest stress. Results indicate that existing forest carbon stocks and functions are moderately persistent and that increased near-term removals may be mistimed for effectively increasing resilience.

KEYWORDS

forest, climate change, modeling, vulnerability, drought, fire, management, carbon

Introduction

Temperate conifer forests are among the most carbon-dense forests globally (Hudiburg et al., 2009, 2019; Thurner et al., 2014; Smith et al., 2019) and are responsible for most of the western North American carbon sink (Schimel et al., 2002). Drought and fire are endemic across much of this region. However, the magnitude of these disturbances has increased in recent decades (Zhao and Running, 2010; Schwalm et al., 2012; Abatzoglou and Williams, 2016; Buotte et al., 2019) due to increased soil and atmospheric aridity, historic harvest impacts, excessive fuels from fire suppression, and human ignitions (Higuera and Abatzoglou, 2021). These shifts have increased the vulnerability of landscape carbon sinks and myriad ecosystem services (Walsh and Hudiburg, 2021). Forest vulnerability to changing drought and wildfire regimes varies among trees, species, and populations (VanderWeide and Hartnett, 2011; Lutz et al., 2012; Evans et al., 2016) due to the interaction between legacies from past disturbance (Hudiburg et al., 2017; Bartowitz et al., 2019) and hotter and drier growing seasons (Allen et al., 2010).

Increasing natural and anthropogenic disturbance in regions of productive, high carbon density forests (Law et al., 2018) has accelerated the need for improved understanding of western U.S. landscape trajectories in the 21st century (Case et al., 2021). Evaluating potential outcomes, however, requires quantifying ecological metrics at appropriate spatiotemporal scales and quantifying trade-offs between management approaches (Hudiburg et al., 2019). Much recent forest management literature emphasizes the need for species composition shifts and density reductions through active management such as harvest and prescribed fire to create more resilient forests (Prichard et al., 2021). Whether or not such actions will successfully decrease forest vulnerability while minimizing carbon losses at landscape scales and across the complex subregions of the western U.S. remains largely untested (Bartowitz et al., 2022). Given the long-term observations needed to empirically confirm the consequences of intertwined novel climate, disturbance, and forest management strategies (Nagy et al., 2021; Muthukrishnan et al., 2022), robust, process-based methods are presently needed to quantify and assess these complex potential outcomes across landscapes and through time (Anderegg et al., 2022). Due to the rapidly changing environmental conditions governing forest growth, mortality, and carbon balance, mechanistic models that explicitly represent forest processes (i.e., photosynthesis, hydraulic limitation, carbon allocation, changes to water use efficiency, prognostic fire events, forest structure, etc.) must be utilized to better predict potential trajectories of forest vulnerability and resulting carbon fluxes of proposed management plans.

Much previous regional-scale forest modeling has utilized two broad categories of models, each with limitations in projecting vegetation responses to novel conditions. First, the land components of earth systems models (ESMs) have represented mechanistic biophysics and biogeochemistry at soil-plant-atmosphere surfaces (Bonan, 2008, 2019), but have historically represented site vegetation via aggregated pools and fluxes of mass (e.g., Hudiburg et al., 2013). Previous studies using ESMs at the scale of western U.S. forests have derived forest vulnerability indicators from model outputs such as site carbon fluxes (e.g., NPP; Buotte et al., 2019), yet their lack of modeled individual mortality and canopy gap formation has meant that key structural feedbacks (e.g., functional gaps, demographics) to projection outcomes were absent. Second, vegetation demographic models (VDMs) have represented structural and compositional shifts of individuals, cohorts, and successional patches across grid cells via mortality and growth (Scheiter et al., 2013). VDMs can lack the spatial scale and biogeophysical dynamics of ESMs, while employing simple empirical representations of essential plant processes (Hanbury-Brown et al., 2022). More recently, coupling of VDMs with ESMs has enabled progress towards regional modeling experiments that fuse mechanistic surface exchanges with ecosystem demographic resolution (Fisher et al., 2018; Fisher and Koven, 2020). These coupled models can enable essential sub-grid cell vegetation heterogeneity via cohorts of trees across variably disturbed patches within the land models of ESMs.

The U.S. Northern Rocky Mountain (NRM) ecoregion (Omernik and Griffith, 2014) represents a important, sparsely studied and carbon dense forested domain (Walsh and Hudiburg, 2021) on which to test advances in coupled forest-disturbance modeling is the western U.S. The NRM contains over 100,000 km^2 of predominantly conifer forests in northern Idaho, Montana, and Washington that have experienced profound 20th and 21st century changes to composition and structure from harvest, insects, pathogens, wildfire, and fire suppression (Bollenbacher et al., 2014; Ramsfield et al., 2016). The NRM was notably the primary region of the 1910 "Big Burn," in which over 1.2 million hectares of wildland burned (Koch, 1942, 1978; Bartowitz et al., 2022). The 1910 fires shaped both NRM forest structure as well as the subsequent fire suppression policies of the nascent United States Forest Service (USFS), which contributed to large reductions in regional burned area by the latter portion of the 20th century (Arno et al., 2000; Gibson and Morgan, 2005; Walsh and Hudiburg, 2021). NRM forests are also imprinted with the legacy of 20th century timber harvest, which ultimately increased tree density and homogenized forest composition with early 20th century selective harvest (i.e., "high grading") followed by even aged, regeneration harvest methods (e.g., clear cutting) (USDA, 2015, 2019).

Critically, much of the present-day NRM region has been identified as a high priority for carbon storage reserves due to higher carbon density than drier regions of the western U.S. and moderate vulnerability to drought and fire mortality (Buotte et al., 2020; Law et al., 2022). However, a warming climate, increased wildfire activity (Parks and Abatzoglou, 2020), and lack of species tolerant to fire, drought, and pathogens relative to the past (Evangelista et al., 2011; Stevens-Rumann et al., 2017; Turner et al., 2019), have led to concern regarding regional 21st century forest vulnerability and continued ability to provide ecosystem services, including the ability of forests to sequester and store carbon (Henne et al., 2021; Walsh and Hudiburg, 2021). In this context, recent national forest land management plan revisions and draft revisions within the NRM aim to reduce forest vulnerability via changes to species composition and density, in part via increased even-aged timber harvests (i.e., harvests that remove the majority of overstory trees) (USDA, 2015, 2019). Increased harvests are incorporated into plans to reduce forest density and sharply increase the prevalence of planted fire, drought, or pathogen-tolerant species (e.g., ponderosa pine, western white pine, and western larch over Douglas fir and mesic mixed conifers). Notably, the draft plan revision for the

Nez-Perce Clearwater National Forest presents multiple alternative scenarios in which sharp increases in even-aged harvest (i.e., up to 3–4 × 2010–2020 timber harvest volumes) are utilized to alter forest composition on the scale of 100,000–300,000 acres per decade (USDA, 2019). In combination, the significant impacts to NRM forest ecosystems from novel climate, natural disturbances, and human disturbances drive a need for the study of potential 21st century landscape function and vulnerability.

Here, we demonstrate a novel approach to modeling 21st century NRM forest vulnerability to loss of biomass and function resulting from climate change and disturbance using CLM-FATES (the Community Land Model with the Functionally Assembled Terrestrial Ecosystem Simulator; Fisher et al., 2015; Lawrence et al., 2018), a cohort-based VDM (FATES) coupled to an ESM (CLM). We employ CLM-FATES due to the model's prognostic mortality mechanisms (fire, carbon starvation, hydraulic failure, and freezing); due to its representation of cohorts of trees with crown spatiality and mass allocated to cohorts with distinct individual counts, species, and organ sizes; and due to its sub-grid cell patches that represent areas of distinct disturbance, functional gaps, and recovery. In this study, modeled NRM forest trajectories from 2025–2100 are assessed via forest mortality, growth, canopy cover, carbon stocks, and carbon fluxes under changing climate, fire, and management. We examine outcomes under both business-as-usual (BAU) scenarios and increased harvest scenarios based on current U.S. national forest management plans in the NRM region. Modified management scenarios include increased regeneration harvest rates that are intended to reduce forest vulnerability to disturbance via prescribed shifts in forest structure and composition. We ask:

1. Does climate change diminish landscape carbon stocks and forest cover in the NRM through 2100?
2. How do changing climate and disturbance impact ecosystem stress, production, and mortality across forest types?
3. Do prescribed composition shifts via increased regeneration harvest (active management) effectively reduce landscape vulnerability to climate change?

Materials and methods

Modeling framework

Simulations were performed with the Functionally Assembled Terrestrial Ecosystem Simulator (FATES; Fisher et al., 2015) coupled with the Community Land Model 5.0 (CLM; Lawrence et al., 2018) of the Community Earth Systems Model (CESM). With this configuration, FATES modifies CLM vegetation surface representation to include vegetation demographics via cohorts of trees occupying patches defined by disturbance history. CLM represents land surface biogeophysics, biogeochemistry, and human land impacts across gridded domains. FATES has been tested and evaluated for sensitivities, parameterization strategies, and predominantly site-scale analyses (Koven et al., 2019; Lawrence et al., 2019; Huang et al., 2020; FATES Development Team, 2022; Lambert et al., 2022).

Functionally Assembled Terrestrial Ecosystem Simulator cohorts represent groups of trees defined by common size, canopy position, and plant functional type (PFT). Cohort processes include photosynthesis, respiration, transpiration, recruitment, growth, reproduction, and mortality driven by climate, light, soil moisture, and disturbance. Cohorts occupy patches within each site that are generated by disturbances. PFTs are defined by common sets of functional traits that correspond to physiology and structure. Surface processes are calculated at a half-hourly time step and include soil-leaf-atmosphere exchanges (e.g., mass and energy fluxes; photosynthesis, respiration, transpiration). Daily time-step processes include recruitment, growth, disturbance, turnover to surface and soil pools, and cohort/patch fusion/fission. Within patches, cohorts compete for light via vertical canopy position (layer), dependent on tree height and total crown area per patch. Net Primary Production (NPP) is the balance between photosynthesis and autotrophic respiration. Growth is in turn dependent on a NPP allocation scheme in which tissue turnover and carbon stores are first replenished, allometric deficits are diminished, and then, if possible, tissues grow concurrently according to allometric targets. Event-based mortality can result from prescribed harvest and prognostic fire impacts mediated by cohort size, bark thickness, and canopy variables. 'Treefall' mortality includes hydraulic failure, carbon starvation (based on carbon balance), cold stress, and a background mortality rate per PFT. Within FATES, a SPITFIRE-based model (Thonicke et al., 2010) simulates daily patch fire initiation, ignition, spread, intensity, and effects based on lightning strikes (here, spatially variable), patch fuel conditions (mass, size distribution, moisture), fire weather, and cohort characteristics (FATES Development Team, 2022; "FATES SPITFIRE description" in the **Supplementary material**).

We modified FATES to enable several processes that were important in our study scenarios (full description in the **Supplementary material**). Modifications included the following: (1) the addition of regeneration harvest as a management option (e.g., harvest and then planting of selected PFTs) and the addition of parameters controlling combustion fraction of harvest slash; (2) the addition of standing dead (i.e., "snag") pools and treefall fluxes to better reflect post-mortality fuel structure and emissions timing (Edburg et al., 2011; Stenzel et al., 2019); (3) the addition of cohort fine root depth based on tree size and PFT to differentiate soil water access based on tree structural growth and PFT strategy (Law et al., 2003; Irvine et al., 2004, 2008; Law and Berner, 2015); and (4) the inclusion of cold stress mortality thresholds for small trees and the calculation of cold stress from daily minimum temperatures, rather than averages. Modifications 3 and 4 were intended to better generate PFT fundamental niches by representing recruit mortality from extreme conditions.

Terminology

Carbon cycle terms include Gross Primary Production (GPP), Autotrophic (plant) respiration (R_a), Heterotrophic respiration (R_h) and Net Primary Production (NPP = GPP–R_a) (Chapin et al., 2006). The balance of ecosystem production and respiratory fluxes define Net Ecosystem Production (NEP = NPP–R_h). The

Net Ecosystem Carbon Balance (NECB) represents the total site carbon balance, subtracting from NEP any additional horizontal fluxes and vertical non-respiratory fluxes (here, NECB = NEP–fire C emissions–harvest removals). Crown area refers to the ratio of forest canopy cover to ground area. Soil moisture stress, used here in place of the CLM-FATES variable "β-Transpiration," refers to model stress-response scaling (0–1) of stomatal conductance and photosynthesis based on soil water matric potential and plant wilting point (FATES Development Team, 2022). Carbon use efficiency (CUE) is the site ratio of GPP to NPP and reflects the efficiency with which modeled photosynthate from GPP is converted to live biomass pools (vs. plant respiration).

Study domain and forests

Simulations were performed within ∼ 2.5 million hectares of US national forest land in the Northern Rocky Mountain (NRM) ecoregion and the northern portion of the Idaho Batholith ecoregion of Idaho (**Figure 1**; hereafter referred to simply as NRM; Omernik and Griffith, 2014) through the year 2100. We focus on the Idaho Panhandle (IPNF) and Nez-Perce Clearwater National (NPCNF) forests due to their recently revised or in-revision forest management plans, which seek desired conditions of altered forest composition in the context of changing climate and disturbance.

The study domain (**Figure 1**) ranges in elevation from ∼450–2,500 m, rising primarily from west to east. The climate of the region is spatially complex; climatic gradients (warm-dry to cold-wet) correspond to strong elevation gradients and latitude, but climate generally consists of relatively dry summers and a maritime influence that leads to high forest productivity compared to drier portions of the Rocky Mountains to the south. The western side of the ecoregion is characterized by a stronger maritime influence, and the domain includes Koppen climate zones Dsb, Dsc, Dfb, and Dfc (Mediterranean-influenced and continental warm-summer and subarctic climates). Much of the domain experiences growing season drought. July, August, and September are typically both the hottest and driest months (**Figure 1**); during this dry period, precipitation is often less than 10% of the yearly total. Forest soil moisture typically decreases to multi-month minimums by the month of August, while tree sap flow, secondary growth, stomatal conductance, and leaf water potential demonstrate marked downregulation and stress (Baker et al., 2019; Stenzel et al., 2021).

The NRM of Idaho is 88% forested, with the largest portion of forest land administered by the US Forest Service (USFS) (Walsh and Hudiburg, 2019). The pre-20th century forest landscape experienced ∼ 50% mixed fire regimes, with lesser proportions of non-lethal and stand-replacing events, but modern regimes have been altered by combinations of fire suppression, timber harvest, and climate (Arno et al., 2000; Morgan et al., 2008; Naficy et al., 2010). Study plant functional types (PFTs) correspond to forest type distributions from previous CLM studies (Buotte et al., 2019), and include types defined by both single and multiple species. PFTs include ponderosa pine (PP, *Pinus ponderosa*), Douglas fir (DF; *Pseudotsuga menziesii*), mixed mesic fir/cedar/hemlock (MC; Douglas fir; grand fir, *Abies grandis*; western redcedar, *Thuja plicata*; western hemlock, *Tsuga heterophylla*), lodgepole pine (LP; *Pinus contorta*), and subalpine fir/spruce (SF; *Abies lasiocarpa*, *Picea engelmannii*). Grand fir and Douglas fir represent ∼ 50% of tree mass in the domain (USDA, 2015, 2019; Walsh and Hudiburg, 2021), dominating warm and cool moist sites. Cold site forests are composed of subalpine Spruce/fir and lodgepole pine types.

Historical timber harvest on the two national forests increased rapidly in the mid 20th century, peaked at over 30,000 acres per year by the 1980s, then declined to an average of ∼5,000 acres per year after 2000 (USDA, 2022). In the first half of the century, high-grade harvests often selectively removed large and commercially valuable trees (Gruell, 1982, 1983; Smith and Arno, 1999; Brown et al., 2004; Naficy et al., 2010). Beginning in the 1950s and until the 1980s, even-aged harvest (e.g., clear cuts) increased drastically on USFS lands. Combined with white pine blister rust, regeneration harvest methods served to increase the prevalence of species such as Douglas fir and grand fir, while western white pine (*Pinus monticola)* was nearly eliminated from the landscape (USDA, 2015, 2019).

Historically, large portions of forest within both present-day national forests burned in wildfires, including the >5,000 km^2 "Big Burn" of 1910 (Bartowitz et al., 2022). Modern burned area has been relatively low in the Idaho Panhandle National forest, with < 300 km^2 (<2.5%) total burned area from 1985–2020 (Eidenshink et al., 2007). In the Nez Perce-Clearwater National Forest, ∼ 3600 km^2 (∼ 22%) of forest area has burned during the same period. In the 21st century, harvest has replaced fire as the primary stand-replacing agent in the Idaho panhandle despite annual timber harvest that is an order of magnitude lower than its 20th century maximum (USDA, 2022). To the south, in the Clearwater Basin of north-central Idaho, >20% of forest area was within burned perimeters from 2000–2019 (Finco et al., 2012; Picotte et al., 2020). In both areas, root diseases from fungi (e.g., *Armillaria*, laminated root rot) are estimated to represent the largest source of non-stand replacing turnover and afflict the greatest areas of Douglas and grand fir forests (USDA, 2015, 2019). Beetle mortality has had the greatest effect on lodgepole pine (mountain pine beetle) in the NRM, though mortality rates are generally lower than in Montana, Colorado, and Wyoming (Berner et al., 2017).

The USFS completed a revised forest management plan for a portion of the NRM (Idaho Panhandle National Forest; IPNF) in 2015, while a second plan for the Nez Perce-Clearwater National Forest (NPCNF) is currently in draft form (USDA, 2015, 2019). Both plans stress that regional forests deviate from historical and desired structure and composition. Revision plan desired conditions aim to increase forest resilience to climate change, including direct (fire, drought) and indirect (susceptibility to insects, pathogens) impacts on tree mortality and growth rates. Desired conditions from the management plans of both national forests include sharp composition shifts, increasing the prevalence of early seral, shade intolerants (e.g., pine species) that can have higher tolerance to fire, drought, windthrow, and/or root disease than more shade-tolerant, mid or late seral mesic forest species.

Desired composition changes include large decreases in Douglas fir and grand fir forest types (USFS definition: USDA, 2019) and increases in ponderosa pine types at warm-dry and warm-moist sites. In the 2019 draft environmental impact

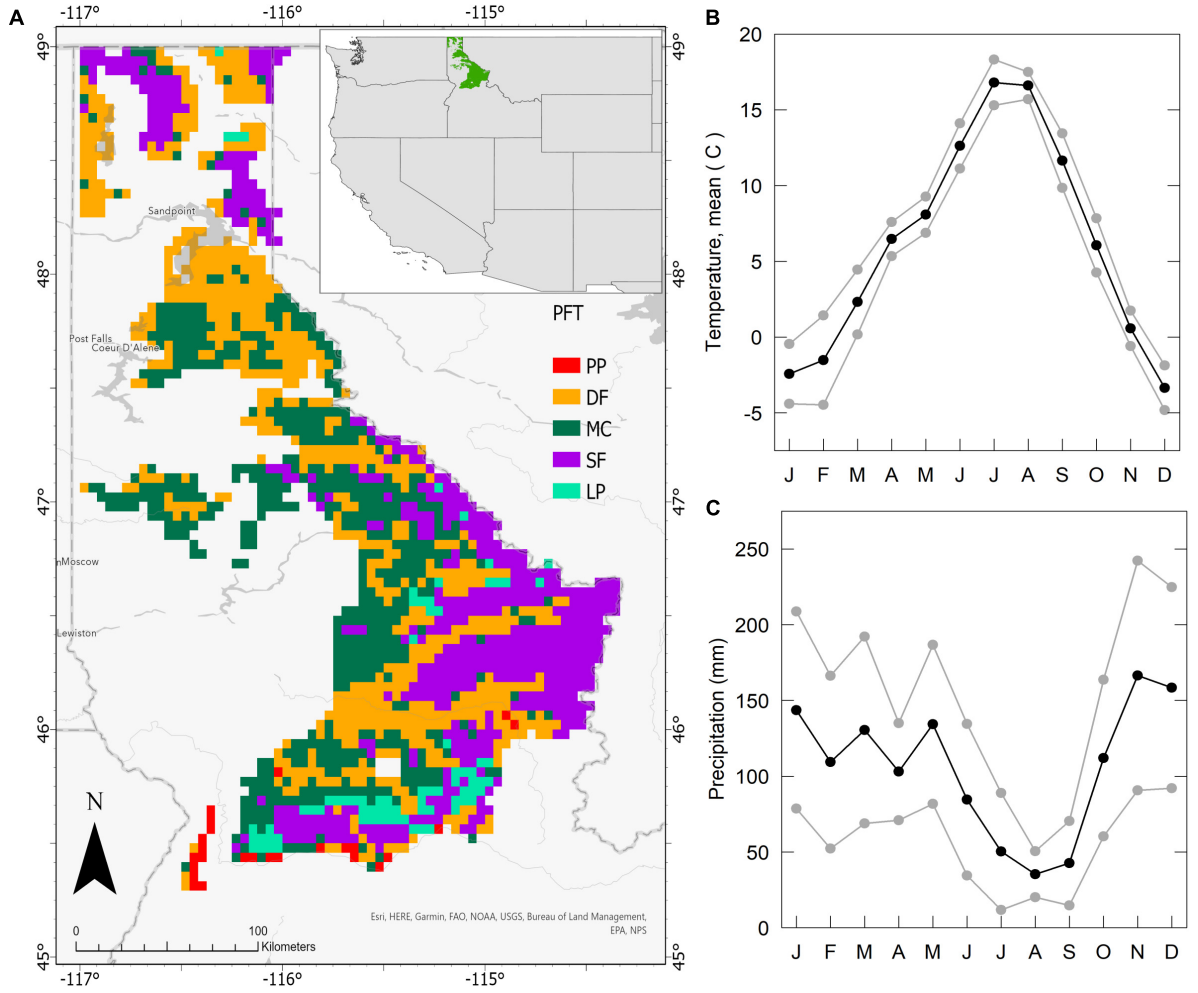

FIGURE 1
Domain location, PFTs, and monthly near-future climate (2025–2035, MIROC climate). **(A)** Domain 4 × 4 km grid cells (n = 1,811) and initial Plant Functional Type (PFT) distribution. PFTs include ponderosa pine (PP), Douglas fir (DF), mixed mesic conifer (MC), subalpine fir and Engelmann spruce (SF), and lodgepole pine (LP). The domain is located in the Idaho Panhandle and Nez Perce–Clearwater National Forests of northern Idaho, USA (see inset). **(B)** MIROC5 mean (± sd) monthly temperature (2025–2034) and **(C)** precipitation.

statement for the NPCNF, for instance, desired conditions include 75–90% and 70–85% reductions in Douglas fir and grand fir/western redcedar forest types for warm-moist sites, which support the largest and most productive forests sites in the region (vs. warm-dry and cold). For the same sites, increases in ponderosa pine forest types of 400–900% are desired. Across NPCNF draft plan alternatives, these conditions would be sought in part with timber harvest increases of ∼40–400% across alternative scenarios (up to 55,000 ha yr^{-1}).

Parameterization

PFT trait data

Tree species trait data informing FATES PFT parameter ranges included observations from the tree trait database compiled in Buotte et al. (2021), the TRY Database (Kattge et al., 2020), the NACP TERRA-PNW Forest database (Law and Berner, 2015), and additional literature (see also attached parameter reference file; Hudiburg et al., 2009, 2013; Buotte et al., 2019).

Parameter selection

For each FATES PFT, we generated parameter set ensembles in which key functional traits were varied within observed ranges (Buotte et al., 2021). To further constrain parameter value, PFT competitive strategies were defined (**Supplementary Table 1**) and final parameters across PFTs were constrained by relative differences in strategies. Where PFT-specific observations were not available, parameters were generally held constant between species.

We first generated 72-member parameter set ensembles for each of 3 generic PFTs, corresponding to a range of tree ecological strategies within the study domain (**Supplementary Table 1**). Initial PFTs included: (1) A shade-intolerant, drought-avoidant, fire-resistant PFT (PINE; corresponding to ponderosa pine forest); (2) A more shade-tolerant, less drought-tolerant, less fire-resistant PFT (FIR; corresponding to regional mesic mixed conifer forest); and (3) A cold-tolerant, fire-intolerant PFT with subalpine canopy architecture (SUB; corresponding to subalpine fir/Engelmann spruce forest). We first defined parameters that would not vary in ensembles (e.g., PFT wood density, stem allometry). Next, key PFT

parameters were varied to represent the range of PFT strategies (**Supplementary Table 1**). Fire resistance was determined by bark thickness (*bark*) and canopy height allometry (*canopy_ht*). Shade tolerance was determined by specific leaf area at the top of the canopy (SLA_{top}), maximum specific leaf area (SLA_{max}), maximum rate of carboxylation (V_{cmax}), leaf nitrogen stoichiometry (*Leaf_N*; affects leaf respiration), leaf biomass allometry (*d2bl1*; affects leaf respiration and LAI), and leaf longevity (*leaf_life*; impacts foliage turnover replacement costs and availability of carbon for structural growth under low carbon-supply conditions). Drought avoidance was controlled by the soil matric potential of stomatal closure (*SMPSC*), stomatal slope (stoma; affects water use efficiency via regulating stomatal conductance in relation to photosynthesis, soil moisture stress, and VPD), and minimum and maximum fine root depth (*root_min*, *root_max*; also affects the rate of root depth growth). Cold tolerance was determined by the seedling cold temperature threshold (*cold_tol_seedling*). SUB PFT crown area (*d2ca*) was decreased relative to PINE and FIR, though we note that FATES does not include mechanics that make narrow, dense tree crowns advantageous due to snow or wind effects. Each initial ensemble member parameter set was generated through random selection of each parameter within a uniform distribution spanning each parameter's observed range.

Calibration

Iterative 72-member single-PFT ensembles for the initial 3 PFTs were run for 150–400 years each across three core sites. Core sites (single grid cells) were characterized by varying ratios of precipitation to potential evapotranspiration (P: PET) and included DRY, WET, and moderate moisture (MOD) sites. PFT ensembles members were filtered (i.e., selected for or against) according to a series of ecological expectations at each site [based on Buotte et al. (2021); see **Supplementary Table 1** for expectations; **Supplementary Figures 18–22** for example results]. The DRY site (PET > P) filtered PFT capability for drought avoidance/tolerance, including the ability of shallow-rooted recruits to avoid carbon starvation or hydraulic dysfunction, and the ability of mature forest to maintain near-canopy closure in the absence of mass disturbance events. At the MOD site (PET ≈ P), PFTs were filtered based on successful formation of near-closed forest canopies under higher site moisture availability than the DRY site. Yearly hydraulic failure mortality of mature trees was selected against. At the WET site (P < PET) carbon starvation mortality was selected for in shade-intolerant PINE PFT recruits under shade-intolerant (and low LAI) FIR PFT canopies. Partial survival and growth of shade-intolerant FIR recruits under low-LAI PINE canopies was selected for. All PFT ensembles were also calibrated to estimated ranges of local biomass by stand age, and carbon fluxes (GPP, NPP) where relevant monitoring ground-based data existed (Law et al., 2001a,b; Irvine et al., 2004; Sun et al., 2004; Stenzel et al., 2021; **Supplementary Figures 18–22**). To develop the final five domain PFT parameterizations (i.e., non-generic; PP, MC, DF, LP, SF), ensemble members that passed initial ecological filters were varied relative to observed ranges for common component species, maintaining PFT-relative parameter relationships. All parameterizations were again evaluated against C stock and flux filters at each site.

Sub-regional wildfire calibrations proceeded with 72-cell simulations. Six (6) grid cells were randomly selected for each of 12 PFT x climate type combinations. For grid cells of each PFT (n = 5), climate types (2–4 per PFT) were assigned via multivariate cluster analysis (Multivariate Clustering, Arcgis Pro; Scott and Janikas, 2009) with mean annual precipitation, T_{min}, and T_{max} from 1979–2014 historical input climate data (Abatzoglou, 2013; Buotte et al., 2021). Wildfire calibration assessed the sensitivity of FATES SPITFIRE to parameter variation, ultimately focusing on variation to the 'drying ratio' parameter (personal communication P Buotte; Thonicke et al., 2010). Final PFT parameterizations were selected by area burned per forest type for the period of 2001–2020 compared to observation-based burn area (Eidenshink et al., 2007; Finco et al., 2012; Picotte et al., 2020). Parameterizations were additionally selected to be within one standard deviation of FIA-based PFT-average aboveground live tree carbon density (Hudiburg et al., 2019) for the period of 2007–2016 and to maintain the relative order of observed stock densities across forest types.

Regional scenarios

Domain-scale scenarios were run across 1811, 4 × 4 km grid cells (∼28,000 km^2 of national forest land) for 600 years each (400-year spin-up, 200-year historical and future from 1900–2099). Six future scenarios (**Table 1**) were run from 2020–2099 and were defined by regionally warmer and cooler RCP 8.5 climate forcings for each of three timber harvest intensities (business-as-usual, moderate harvest increase, high harvest increase; see detailed descriptions below).

Surface datasets defined land variables, including soil texture, color, slope, depth to bedrock, and PFT area distribution (from Lawrence et al., 2018; Buotte et al., 2021). FATES 'fixed biogeography' mode was enabled and a single initial PFT was prescribed per site based on Buotte et al. (2019) dominant gridcell PFTs (by area). Fixed biogeography mode was selected because the aggregated soil water pools within and across patches in CLM FATES limit spatially variable impacts of different soil water use strategies across multiple site PFTs (see discussion section) in the seasonally dry domain. For each scenario, FATES mass stocks and fluxes were spun-up for 400 years under repeated historical climate (1950–1979). This spin-up period length was sufficient for all PFTs to reach equilibrium ecosystem carbon stocks (live and dead tree, soil C), fluxes (NPP, GPP, R_a, R_h) and site dynamics (crown area, mortality, size structure) under a recycled 30 year climate. Domain live tree, litter, and woody debris pools each changed by ≤ 1% across the final 100 years of spin-up. Soil C stocks increased by ∼0.1% yr^{-1} by spin-up year 400. Historical and then future periods were simulated with 1950–2099 climate inputs (see climate details below).

Historical harvest fraction by grid cell and year was prescribed via the CLM "land-use timeseries" harvest dataset according to USFS records (**Supplementary Figure 2**; Hurtt et al., 2020; USDA, 2022). Currently, FATES does not allow spatiotemporal variation in selective harvest parameters that interact with CLM harvest areas. We therefore prescribed harvests that removed the overstory ("clearcuts") within dynamic harvest areas, both with and without planting. While this represents a simplification of

10.3389/ffgc.2023.1146033

TABLE 1 Future regional scenarios.

Name	RCP	Description	CO2	Source	
Climate					
MIROC	8.5	'Cooler'. From MIROC5 GCM. 1/24° (4 km), 3 h.	Constant, yr 2000	Buotte et al., 2019	
IPSL	8.5	'Warmer'. From IPSL-CM5A-MR GCM. 1/24° (4 km), 3 h.	Constant, yr 2000	Buotte et al., 2019	
Name	**Description**	**Area (ac yr^{-1})**	**Distribution**	**Methods**	**Source**
Timber harvest					
BAU	Business-As-Usual	~ 4,500	2001–2020 grid cell harvest proportions	Regen Harvest, only stands with cohorts > 20 cm DBH	USDA, 2022
AC1	Moderate Harvest Increase	~ 12,000	2001–2020 grid cell proportions, redistributed if > 100% by 2100	see above	USDA, 2015, USDA, 2019 scenarios "W" and "X"
AC2	High Harvest Increase	~ 23,000	2001–2020 grid cell proportions, redistributed if > 100% by 2100	see above	USDA, 2015, USDA, 2019 scenarios "W" and "X"

Six 2020–2099 scenarios were simulated from 3 timber harvest intensities under each of 2 climate forcings. Values indicate mean (sd) of 1811 gridcell decadal means, with single years referring to decadal end years (e.g., 2029 for 2020–2029). The dead C pool aggregates aboveground (litter, woody debris, snag) and belowground (fine and course roots) dead biomass. Drought mortality is the sum of hydraulic failure mortality and carbon starvation mortality.

actual harvest prescriptions experienced on the landscape, harvest records (USDA, 2022) indicate that less than 25% of regional harvests from 2001–2020 were selective. Further, while additional even-aged techniques were not represented (e.g., shelterwood, seed tree), many of the regeneration benefits those techniques provide (seeding, protection from plant competition) are realized by seedlings in FATES regardless.

Based on USFS management plans from the Idaho Panhandle and the Nez Perce-Clearwater National forests, future harvest scenarios were generated to represent business-as-usual (BAU; from 2001–2020 harvest averages; ~ 4,500 acre yr^{-1}), moderately accelerated harvest (AC1 ~ 12,000 acre yr^{-1}) and highly accelerated harvest (AC2; ~ 23,000 acre yr^{-1}). AC1 and AC2 primarily reflect variable potential contributions from the NPCNF draft forest plan scenarios "W" and "X," and were calculated from estimated timber harvest production (USDA, 2019). For all harvest scenarios, yearly grid cell harvest area as a proportion of yearly domain harvest followed observed cell harvest proportions from 2001–2020 (USDA, 2022). In cases where >100% of grid cell area would be harvested during the 2025–2100 future simulations due to increased rates, harvest area above 100% was allocated to cells with <100% period harvest. As with historical prescriptions, even-aged harvests were prescribed in the future. Both forest revision plans list regeneration harvest and selective harvest as "possible actions." However, given the large desired species composition shifts and a modeled dependence on regeneration harvest methods in the Nez Perce-Clearwater plan (USDA, 2019), non-selective harvests were simulated. To represent even age regeneration harvest practices rather than selective harvest, FATES code was modified to only harvest on patches that contained cohorts of trees with > 20 cm DBH. For forest pixels that had not been classified as cold-wet or cold-dry during calibration (from calibration climate-type analysis), non-BAU harvest scenarios implemented regeneration harvest-based composition shifts via planting of the PP PFT following harvest.

Two future climate scenarios were defined by 1/24° × 1/24° (~ 4 km × 4 km), 3-hourly climate input data derived from the MIROC5 (MIROC) and IPSL-CM5A-MR (IPSL) general circulation models under historical and RCP 8.5 greenhouse gas concentrations (1950–2099) (Abatzoglou, 2013 (datasets from Rupp et al., 2017; Buotte et al., 2019). The climate data was previously downscaled and disaggregated to force 4 × 4 km CLM 4.5 simulations. RCP 8.5 climate forcings were selected due to similarity to global emissions trajectories (Peters et al., 2013; Buotte et al., 2019). The two climate models were selected due to necessary variable availability and continuity. Regionally, future MIROC climate is cooler and wetter than IPSL climate (**Supplementary Figure 1**; see Buotte et al., 2021 supplemental information for detailed climate model comparison and dataset methodology). The 4 × 4 km inputs included air temperature, humidity, incoming solar radiation, windspeed, and precipitation. Scenarios were forced by transient climate but constant CO_2 (year 2000). During initial study simulations and under constant climate, transient CO_2 experiments led to > 50% increases from equilibrium live PFT biomass in 50–100 years, also disrupting PFT strategies that had been defined via PFT calibration (e.g., shade-intolerant pine began to survive under full canopy cover). Excessive CO_2 fertilization relative to observations was possibly the result of the current FATES version not representing gross and primary production limitations aside from those associated with carbon and water supply (e.g., only representing carbon cycling, excessive C

supply invariably resulting in increased structural growth; Körner et al., 2005; Anderson-Teixeira et al., 2013).

FATES SPITFIRE was driven by spatiotemporally variable forest processes (prognostic) and climate (prescribed). A future natural (lightning, 0.5°, 3-hourly) ignitions dataset was repeated yearly and based on 1995–2013 averages. Human population density (0.5°) from the year 2000 drove future human ignition rates. Fire suppression has not been implemented in CLM FATES to date; we implemented a constant fire area suppression factor (0.61) in non-wilderness grid cells based on CLM5 socioeconomic suppression formulas for the region (from population density and GDP; Lawrence et al., 2019). For additional details on FATES SPITFIRE dynamics and documentation references, see the Supporting Material section "FATES SPITFIRE description."

Model outputs were scaled by percent forest cover to account for non-forest regions within the actual domain (Ruefenacht et al., 2008). Modeled live and dead carbon stocks across non-calibration grid cells were evaluated per PFT in comparison to FIA-based live tree carbon stock estimates (**Supplementary Table 2**; Gray et al., 2012; Hudiburg et al., 2019). Carbon fluxes were assessed across the domain in comparison to MODIS NPP and GPP within MODIS product grid cells classified as 'Evergreen Needleleaf Conifer' (ENF) (Running and Zhao, 2021). Total modeled burned area was evaluated relative to combined low, moderate, and high severity burn areas recorded from the Monitoring Trends in Burn Severity (MTBS) project for the historical period (Eidenshink et al., 2007). MTBS has known caveats (Kolden et al., 2015) and reflects the full fire suppression strategy employed by USFS, but is the most accurate representation of contemporary area burned.

Results

Model evaluation

Calibration

Final PFT parameter set selections passed all site-scale PFT filters at DRY, MOD, and WET locations (**Supplementary Table 1**) during site calibrations (**Supplementary Figures 18–22**). The DRY site supported recruit establishment of the calibrated ponderosa pine (PP) PFT but not the mesic fir PFT, which faced high hydraulic failure mortality. DRY site PP simulation outputs were within observed variable ranges from local eddy covariance site and chronosequence plots (**Supplementary Figure 21**), including total live tree C across stand ages, NPP, and GPP. At the MOD site, both generic pine and fir PFT were able to successfully initiate, with high NPP and biomass accumulation of young pine stands relative to the DRY site that was within observed ranges (**Supplementary Figure 22**). Due to carbon starvation from light limitation and consistent with site observations, the MOD site did not support a persistent understory. The WET site experienced the highest rates of site biomass accumulation for both PFTs from bare ground (**Supplementary Figure 20**). There, site FIR recruit presence persisted under a PINE canopy, passing the FIR PFT filter of moderate shade tolerance. In the absence of fire or harvest, WET site mean 100-year stand tree C was between FIA plot-based means and maximums for ponderosa pine and mixed conifer forests.

Validation

Across all PFTs, mean modeled aboveground tree C stocks were within one standard deviation of FIA plot-based calculations within the domain (2007–2017 period. Mean modeled: 63–103 Mg C ha^{-1}; mean observed: 53–108 Mg C ha^{-1}) (**Supplementary Table 3**; **Supplementary Figure 17**) and followed the same order of carbon stock densities. Mean modeled subalpine fir/spruce (SF), lodgepole pine (LP), and Douglas fir (DF) tree stocks exceeded FIA-based means by 10, 18, and 22% in 2010. Ponderosa pine (PP) and mixed conifer (MC) means were 4 and 5% lower than observations. Yearly simulated burn fractions for PP, DF, and MC also fell within one standard deviation of MTBS-based averages for the period of 2001–2017 (modeled means: 0.38–2.59% yr^{-1}; observed means: 0.31–2.33% yr^{-1}). SF and LP mean burn fractions of 0.14% yr^{-1} underestimated the observed 1.02% yr^{-1} for 2001–2017 due to inadequate fuel dryness. The 0.14% yr^{-1} 2001–2017 modeled burn fraction was similar to the 1985–2000 rate of 0.15% yr^{-1}. Observed changes to SF and LP burn fractions from the late 20th to early 21st centuries (∼ 1000%) were higher than other PFTs (from MTBS).

In comparison to MODIS GPP estimates of 955–1,117 g C m^{-2} yr^{-1} across PFT site-types, modeled GPP means of 837–1178 g m^{-2} yr^{-1} were 8–18% higher (PP, DF, MC) and 13–24% lower (LP, SF) (**Table 2**; **Supplementary Figure 17**). All MODIS PFT NPP means (558–628 g C m^{-2} yr^{-1}) were higher than modeled NPP (398–495 g C m^{-2} yr^{-1}). As a result, mean MODIS CUE (NPP/GPP) across PFT domains of 0.54–0.59 exceeded modeled CUE means of 0.39–0.48. Nonetheless, modeled CUE ranges overlapped with previously observed ranges for temperate coniferous forests (DeLucia et al., 2007).

Future forests

Across all transient climate and management scenarios, live and dead carbon stocks decreased between 2025 and 2099 (**Table 2**, **Figure 2**). Total domain live tree carbon stocks decreased by 5–29%, with greater losses incurred under the hotter IPSL climate scenarios and with increasing timber harvest. In all scenarios, GPP, NPP, and NECB decreased by the late 21st century (**Figure 3**) due to a combination of: (1) high intermittent mortality from fire, hydraulic failure, and carbon starvation during hot and dry years (**Figures 4–8**) that led to decreases in crown area and GPP but not heterotrophic respiration (**Figures 3**); (2) tree stress from increased VPD and decreased VWC (**Supplementary Figure 1**) that led to decreases in GPP and carbon use efficiency (NPP/GPP; **Figures 3**, **6**); and, (3) decreased replacement of killed crown area due to increased mortality of recruits and decreased allocation to seed biomass as NPP declined (positive feedback) (**Figure 5**).

Within the domain, IPSL 2050–2059 and 2090–2099 mean annual temperature (MAT) was 0.9 and 1.7°C higher than MIROC (**Supplementary Figure 1**). Domain MAT under IPSL and MIROC increased 5.5 C and 3.9 C, respectively, between 2026–2030 and 2095–2099. Future annual precipitation increased in both scenarios before declining from 2080–2090. Relative to MIROC, the hotter IPSL BAU scenario experienced ∼250% greater burned area from 2025–2100 (**Table 2**). Large burned area differences between climate forcings resulted from extreme fire years, particularly from the 2050 and later (**Figure 4**). From 2026–2099, IPSL and MIROC

TABLE 2 Domain forest stocks and fluxes by climate and management scenario.

Climate	Harvest	Period	Tree C	Dead C	Crown area	NPP	NECB	Mortality total	Mortality harvest	Mortality drought	Mortality fire	Burned fraction
			Mg ha^{-1}	Mg ha^{-1}	m^2 m^{-2}	g m^{-2} yr^{-1}	g m^{-2} yr^{-1}	g m^{-2} yr^{-1}	g m^{-2} yr^{-1}	g m^{-2} yr^{-1}	g m^{-2} yr^{-1}	m2 m^{-2} yr^{-1}
MIROC5	BAU	2029	131 (40)	56 (30)	65 (16)	460 (119)	1 (0)	164 (39)	6 (9)	2 (1)	5 (15)	0.16 (0.39)
		2059	133 (40)	54 (29)	66 (16)	463 (121)	−8 (45)	167 (41)	6 (9)	2 (7)	5 (8)	0.17 (0.27)
		2099	126 (39)	51 (28)	61 (17)	349 (107)	−78 (47)	176 (47)	6 (9)	13 (44)	11 (14)	0.31 (0.35)
		2025–2099	132 (40)	54 (28)	65 (16)	428 (114)	−19 (40)	170 (39)	6 (9)	4 (9)	7 (8)	0.2 (0.29)
	AC2	2059	124 (43)	53 (28)	61 (18)	442 (134)	−56 (93)	190 (50)	41 (58)	2 (7)	4 (7)	0.14 (0.22)
		2099	113 (49)	48 (29)	59 (22)	380 (176)	−70 (78)	187 (52)	38 (57)	10 (34)	10 (13)	0.31 (0.34)
		2025–2099	122 (44)	52 (28)	61 (18)	425 (134)	−48 (74)	192 (48)	41 (58)	3 (7)	6 (7)	0.18 (0.24)
	AC1	2059	129 (41)	54 (29)	64 (17)	454 (124)	−30 (58)	178 (43)	22 (34)	2 (7)	4 (7)	0.16 (0.26)
		2099	122 (43)	50 (28)	55 (20)	378 (160)	−66 (70)	184 (49)	22 (35)	12 (40)	10 (14)	0.26 (0.3)
		2025–2099	128 (41)	53 (28)	63 (17)	432 (126)	−30 (51)	181 (42)	22 (34)	4 (8)	7 (8)	0.2 (0.27)
IPSL	BAU	2029	128 (38)	58 (31)	61 (15)	460 (117)	−9 (47)	170 (42)	6 (8)	2 (6)	14 (16)	0.29 (0.27)
		2059	119 (37)	55 (30)	58 (16)	348 (107)	−97 (46)	190 (60)	5 (8)	7 (28)	40 (37)	0.63 (0.49)
		2099	105 (37)	46 (26)	51 (18)	286 (113)	−157 (42)	220 (89)	5 (8)	38 (107)	59 (56)	1.24 (0.71)
		2025–2099	119 (37)	52 (28)	57 (17)	369 (111)	−82 (36)	174 (45)	5 (8)	8 (19)	24 (17)	0.51 (0.34)
	AC2	2059	111 (39)	54 (30)	54 (18)	338 (121)	−132 (77)	208 (61)	37 (53)	6 (25)	37 (36)	0.56 (0.42)
		2099	95 (46)	42 (27)	49 (23)	311 (186)	−152 (77)	216 (85)	35 (54)	23 (75)	53 (55)	1.12 (0.72)
		2025–2099	110 (41)	51 (28)	54 (18)	367 (135)	−108 (66)	192 (51)	38 (54)	6 (15)	22 (17)	0.46 (0.31)
	AC1	2059	115 (37)	55 (30)	56 (17)	344 (113)	−113 (55)	199 (60)	20 (31)	7 (27)	38 (36)	0.6 (0.47)
		2099	102 (42)	44 (26)	51 (21)	311 (170)	−148 (71)	220 (85)	20 (34)	31 (92)	55 (54)	1.19 (0.7)
		2025–2099	115 (38)	51 (28)	56 (17)	373 (126)	−92 (47)	183 (47)	21 (32)	7 (17)	23 (17)	0.49 (0.33)

10.3389/ffgc.2023.1146033

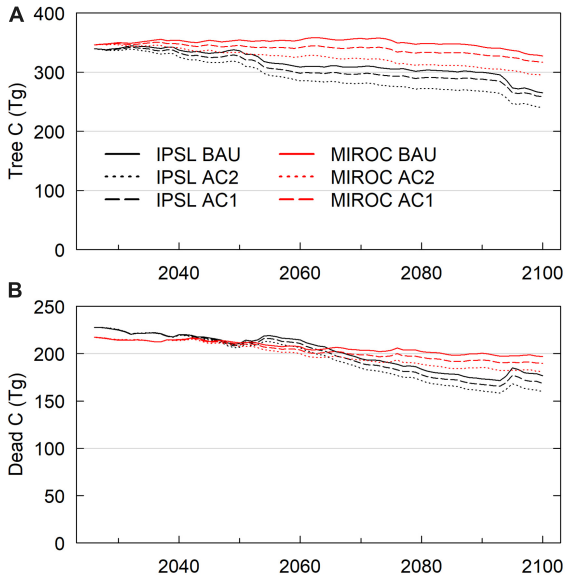

FIGURE 2
Carbon Stocks, 2026–2099 scenario domain averages. **(A)** Live tree carbon stocks. **(B)** Litter and woody debris carbon, above and belowground. Belowground litter and woody debris result from turnover of fine root (to litter) and course root (to woody debris) model pools.

burned areas were ~10,000 km^2 and ~4,000 km^2, or 38% and 15% of domain area. IPSL burned fraction approximately doubled between 2000–2049 and 2050–2099 (~ 0.33% yr^{-1} to 0.6% yr^{-1}), while mean MIROC burned fraction remained consistent (~ 0.22% yr^{-1} to 0.21% yr^{-1}). A lack of strong MIROC burn area increase resulted from large fuel losses to combustion during large early 2000s fire events as well as increases in precipitation that buffered fuel moisture (Figure 4).

Domain climate impacts, business-as-usual

Under BAU management, the hotter IPSL climate scenario experienced earlier and more extreme decreases in carbon stocks, greater burned area, and higher mortality compared to cooler MIROC scenario (Table 2). IPSL scenario live and dead carbon stocks decreased throughout the 21st century, with 24% vegetation C stock decreases between 2020–2029 and 2090–2099 (Figure 2). Extreme fire and drought years resulted in intermittent, sharp declines in live tree carbon. High fire years were associated with a combination of high burn fractions, high fire intensity, and low fuel moisture that overwhelmed negative feedbacks from lower fuel availability (Figure 4). During these acute mortality years, by mass, fire became the dominant source of tree mortality, followed by hydraulic and carbon starvation mortality from drought (Figures 7, 8).

IPSL domain annual NECB declined sharply during the periods of 2020–2050 and 2080–2100, leading to negative NECB after ~ 2030 (Figure 3). Tree crown area, GPP, NPP, and NECB fell following high mortality years (Figure 8) due to greater declines in primary production than heterotrophic respiration. However, across the century, declining VWC (Supplementary Figure 1) also continually depressed NPP, NECB, and CUE via decreased stomatal conductance and GPP (carbon supply relative to autotrophic and heterotrophic respiration) (Figures 3, 6). Decreased forest area and decreased NPP led to decreases in seed production and a resulting 37% decrease in recruitment between 2020–2029 and 2090–2099 (Figure 5). Notably, forest losses stabilized for a period after the mid-century (~2060–2080) due to a combination of increased precipitation (Supplementary Figure 1) and decreased forest cover (Figure 5). Early period mortality resulted in increased moisture availability on a crown area basis (a negative feedback) and decreased moisture stress (Figure 6).

In contrast to the BAU IPSL climate scenario, MIROC BAU live tree C stocks did not begin to decline until the onset of high fire and drought mortality years in the late 21st century (>2075, >2090) (Figures 2, 7). Under this relatively cool climate scenario, domain total tree C stocks instead increased modestly from ~2010–2075 following a gradual decline during the peak harvest years of the mid 20th century. From 2008 –2075, mean live tree carbon pools increased from 126 Mg ha^{-1} to a maximum of 135 Mg ha^{-1} (similar to early 20th century levels). By 2100, live carbon stocks had decreased to 124 Mg ha^{-1}, with a consistent and steep decline from 2085 onwards. MIROC scenario NEP, GPP, and NPP was on average 50%, 17%, and 22% higher than the IPSL BAU scenario during 2090–2099. Early to mid-century increases in MIROC live tree carbon stocks occurred despite gradual increases in autotrophic respiration that drove decreases in NPP, NECB, and CUE (Figure 3). Combined warmer and wetter conditions led to increases in heterotrophic respiration; decreases in litter, CWD, and snag carbon pools; and approximately balanced total domain total carbon stocks (<1% decrease).

The cooler MIROC BAU scenario experienced relatively low fire and drought-related mortality (Figures 7, 8) through much of the 21st century. After the highest mortality year of the 21st century in 2075 (>300% the century average mortality rate), crown area then decreased ~9% through 2100, precipitating a transition to late-century, continual decreases in NPP, GPP, NEP, and live and total carbon stocks (Figures 2, 3).

Both scenarios experienced continual forest biomass declines (Figure 2) by the 2090s due to late century increases in plant water and carbon balance stress (Figure 6). Continual increases in soil moisture stress and temperature decreased stomatal conductance and tree C stores. Stress responses in turn led to decreases in NEP and the first occurrences of years in which drought mortality (carbon starvation and hydraulic failure) became the highest source of prognostic mortality for canopy trees (Figures 7, 8).

Under both BAU scenarios from 2025–2100, the highest mortality rates by tree count resulted from mortality of newly recruited, small trees. In decreasing order, the greatest number of trees were killed by hydraulic failure, background mortality, freezing, and carbon starvation. In contrast, mortality by mass for both IPSL and MIROC climate scenarios (Table 2) resulted most from background mortality (1.4 and 1.7 Mg C ha^{-1} yr^{-1}, respectively), followed by fire (0.24 and 0.05 Mg C ha^{-1} yr^{-1}), harvest (0.04 and 0.05 Mg C ha^{-1} yr^{-1}) and hydraulic failure mortality (0.07 and 0.04 Mg C ha^{-1} yr^{-1}). However, hot and dry year natural disturbance mortality (combined fire, hydraulic failure, and carbon starvation) was responsible for the highest mortality years of the century, which exceeded average rates by maximums of ~300–400% (Figures 7, 8). During these years, the abrupt decreases in live tree mass generated losses of ecosystem GPP and NPP via reductions in crown area. A subsequent lack

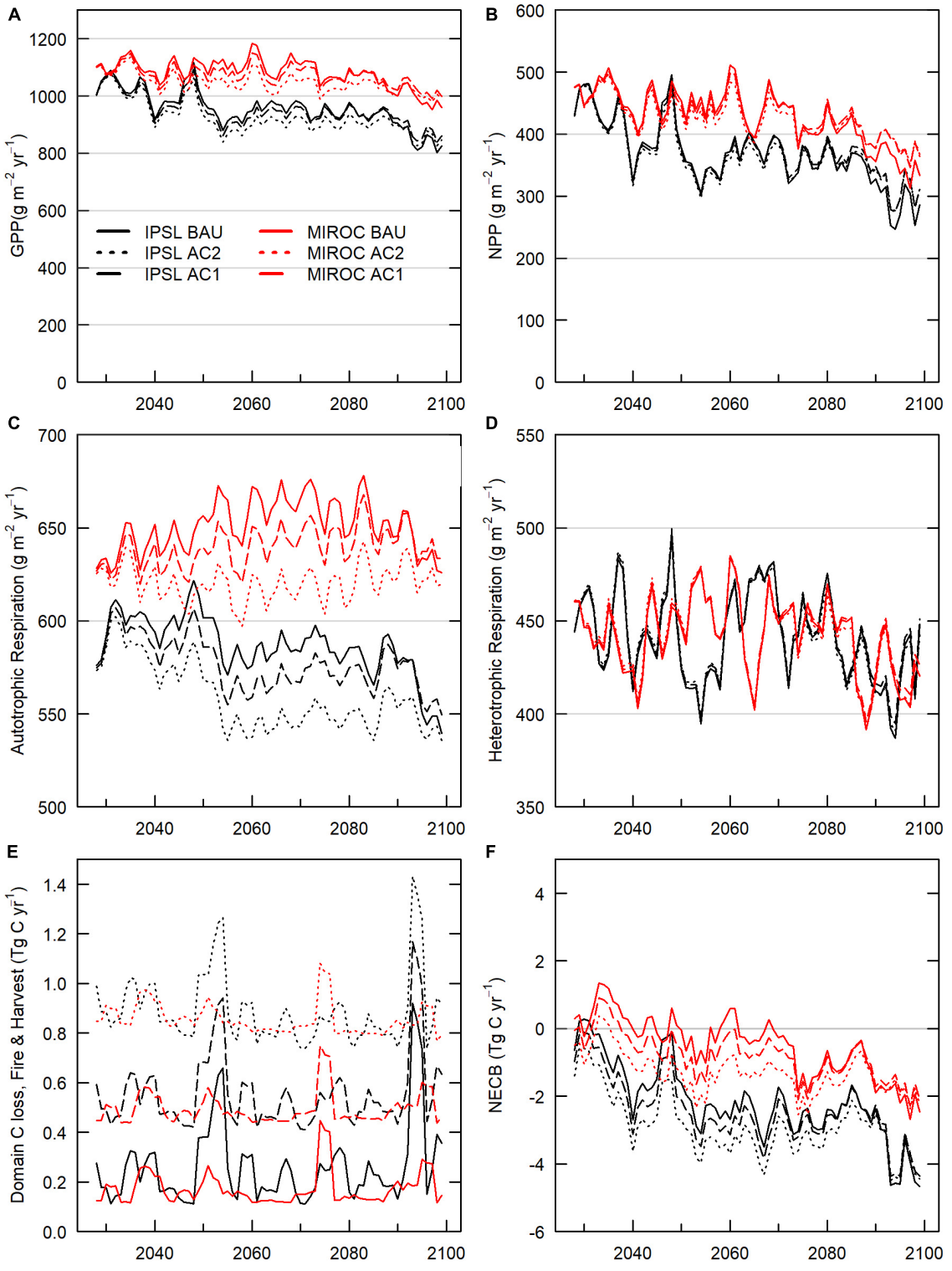

FIGURE 3
Carbon fluxes, 2026–2099 scenario domain averages. **(A)** GPP. **(B)** NPP. **(C)** Autotrophic respiration, **(D)** Heterotrophic respiration **(E)** Domain C losses (outfluxes from domain) from wildfire fire emissions, harvest slash emissions, and harvest removals. **(F)** NECB.

of crown area and primary production recovery resulted from previously depressed NPP, growth, seed allocation, and recruitment rates. IPSL BAU scenario mean and maximum yearly mortality rates (1.5 and 6.3% of live tree mass) exceeded MIROC BAU mortality rates (1.3 and 2.6%).

PFT responses, business-as-usual

Throughout the 21st century, intermittent, acute mortality occurred during high fire and drought years (**Figures 8**, **9**; **Supplementary Figures 12–16**), yet intensified for most PFTs and climate scenarios in the 2090s. As a proportion of live site

10.3389/ffgc.2023.1146033

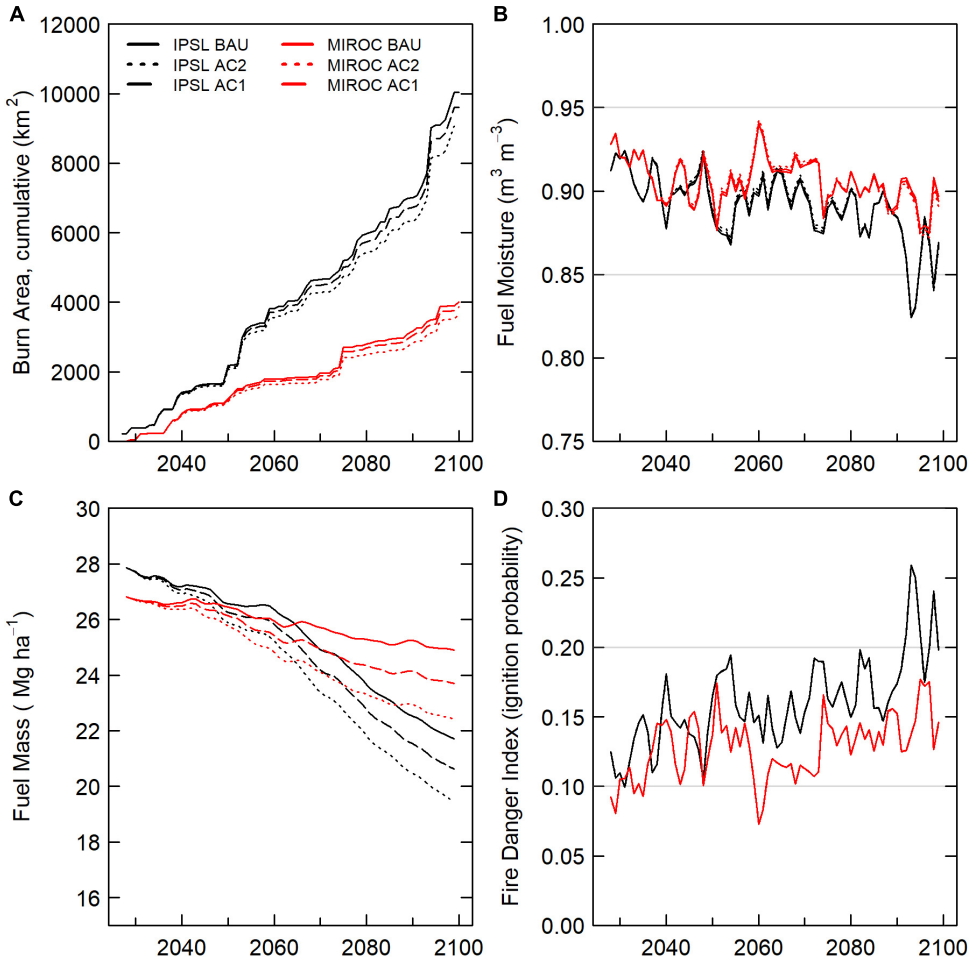

FIGURE 4
Wildfire dynamics, 2026–2099 scenario domain averages. **(A)** Cumulative wildfire burned area by scenario. **(B)** Fuel moisture. **(C)** Fuel Mass. **(D)** Fire danger index.

mass, PFT-average 2090–2099 mortality under MIROC climate increased over 2020–2029 mortality by 4% (PP), 24% (DF), 12% (MC), 8% (SF), and 59% (LP). IPSL climate scenario mortality rates increased by 385% (PP), 106% (DF), 47% (MC), 39% (SF), and 61% (LP). By 2090, all PFTs under both climate scenarios experienced years in which drought-related mortality (hydraulic failure and carbon starvation) exceeded mortality from fire or harvest as temperatures increased, precipitation decreased from mid-century maximums, and VWC decreased (**Supplementary Figure 1**). In contrast, during the spin-up and historical periods, hydraulic failure largely affected shallow-rooted recruits and was not a large source of canopy mortality or mortality by biomass. In the 2090s, dry PP sites were the only site-type on which carbon starvation mortality exceeded hydraulic failure mortality. Despite greater burned area extremes after 2050, average fire mortality and burned area did not continually increase across the century under MIROC climate for DF, MC, and SF and under both climate scenarios for dry PP and LP sites (**Supplementary Figures 3–7**, **12–16**). In contrast, DF, MC, and SF burned area under IPSL climate increased over earlier 21st century burn area maximums by the 2090s.

Average BAU live tree carbon, dead carbon, and crown area decreased across most PFT site types and climate scenarios after 2075 (**Figure 9**; **Supplementary Figures 12–16**). Between 2025 and 2099, PFT-site tree C for IPSL and MIROC scenarios, respectively, decreased by 42% and 9% (PP), 23 and 10% (DF) 17% and 4% (MC), 23% and −1% (SF), and 40% and 14% (LP). Crown cover decreased by 26% and 21% (PP), 21% and 10% (DF), 24% and 11% (MC), 22% and −1% (SF), and 30% and 8% (LP). Litter and woody debris C decreased by 26% and 21% (PP), 21% and 10% (DF), 24% and 11% (MC), 22% and −1% (SF), 30% and 8% (LP). MC, DF, SF, and LP relative tree carbon deficits under IPSL versus MIROC climate continually widened from 2025–2099 (**Figures 2**, **9**).

Between 2025 and 2075, MIROC MC and SF site tree carbon increased modestly (3% and 6%) under moderately warmer and wetter climate (**Figure 9**; **Supplementary Figures 15**, **16**). Continued MC and SF stock growth through the mid century was the result of relatively low R_a and leaf turnover costs, higher NPP, and/or higher allocation to wood versus PP and DF on drier sites. MC and SF stock growth occurred despite comparatively low GPP. Reflecting this trend, MC and SF CUE under IPSL and MIROC decreased by 19% and 18% (MC) and 15% and 13% (SF), while

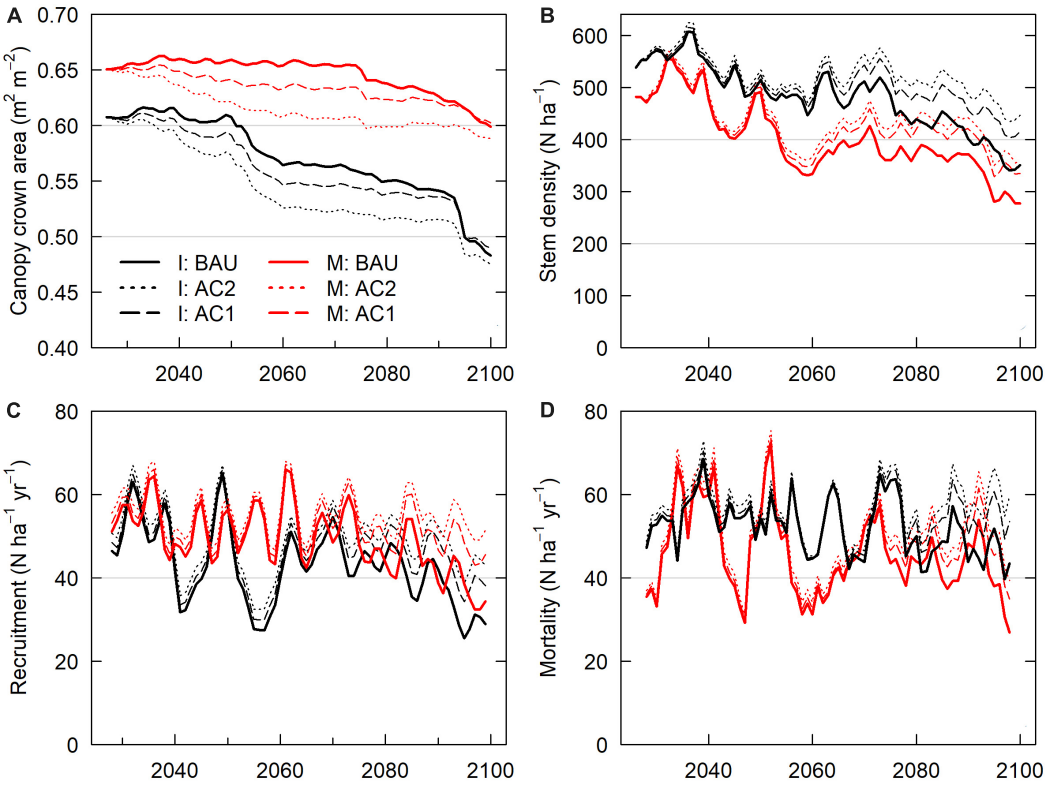

FIGURE 5
Forest structure and turnover, 2026–2099 scenario domain averages. **(A)** Canopy layer crown area. Canopy crown area < 1.0 implies site patches with bare ground. **(B)** Stem density. **(C)** Recruitment of new seedlings from seed stock. Note: Recruitment values include tree planting with regeneration harvest. **(D)** Tree stem mortality.

PP, DF, and LP CUE decreased by 24–31% (IPSL) and 18–28% (MIROC).

Ponderosa pine site C Stocks under the hotter IPSL climate did not decrease below MIROC stocks until the 2050s and then remained 5–10% lower until declining sharply in the 2090s (Figure 9). Despite higher fire and drought mortality, IPSL PP-site GPP, NPP, and crown area did not decline below MIROC values during this period due to higher ISPL PP tree C stocks and NPP In the early 21st century under moderate warming (Supplementary Figure 12).

Management impacts

By 2100, increased harvest scenarios (moderate: AC1; high: AC2) had lowered domain live carbon by 2.5–3.2% (AC1; 6.5–10.5 Tg C) and 9–10% (AC2; ∼ 24–32 Tg C, from 327 Tg C BAU) by 2100 (Table 2; Figure 2; Supplementary Figure 9). Within active harvest grid cells only, 2099 increased harvest tree carbon was 4–11% lower (AC1) and 16–18% lower (AC2) than under BAU. Year 2100 BAU-relative deficits of AC1 scenarios decreased from maximum deficits of 12.4–15.6 Tg C in the 2070s. Increased harvests decreased average crown coverage by ∼ 3–7% during the mid century (Figure 5; Supplementary Figure 10). AC1 harvest scenario crown area then reached approximate parity with BAU scenarios by 2100 due to harvest feedbacks with fire and tree stress (Figure 7). Increased harvest scenarios decreased burn area mortality due to decreased average fuel mass and decreased late-period water stress due to lowered transpiration (higher VWC and lesser downregulation of stomatal conductance). In the 2090s, Increased harvest scenario NECB exceeded that of BAU scenarios (Table 2). Lower 2090s BAU NECB resulted from a combination of lower GPP (higher water stress) and higher R_a (higher live biomass), not higher mortality (Figure 3).

AC2 and AC1 harvest scenarios increased total mortality mass over BAU by increasing harvest mortality (Figures 7, 8), ultimately killing additional tree mass of 18–22 Tg C (AC1) and 37–44 Tg C (AC2) from 2026–2099. Increased harvest scenarios decreased 2026–2100 fire and drought-related mortality (hydraulic failure and carbon starvation) mass by 1.5–4.5 Tg C (AC1) and 2.9–8.6 Tg C (AC2). Burned area was also reduced by 4–9%, with the greatest reduction in the IPSL climate scenario. Decreases in burned area and total mortality resulted from 5–10% decreases in fuel mass (Figure 4) and resulting decreases in fire intensity. Decreases in fuel mass were the result of both the direct removal of live woody biomass that would otherwise have reached dead surface pools and via reductions in site NPP_{wood} and NPP_{leaf}.

Ponderosa pine PFT-site tree and ecosystem C was higher in BAU scenarios than AC2 and AC1 through 2100 (Supplementary Figure 12). However, during high fire and drought mortality years of the 2090s, AC2 NPP at PP sites exceeded that of BAU and AC1 scenarios. AC2 crown area deficits also shrank. For IPSL scenarios near 2100, lower AC1 and BAU NPP resulted from higher canopy mortality. During the 2090s, PP sites first began to experience years in which carbon starvation was the leading source of mortality by mass (Supplementary Figure 3). For MIROC

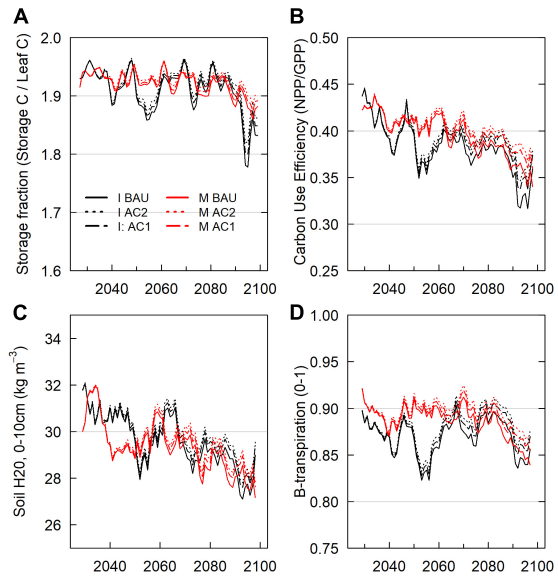

FIGURE 6
Tree stress and efficiency, 2026–2099 scenario domain averages. **(A)** Tree carbon storage as a proportion of leaf carbon. This proportion is used by FATES to determine the onset of cohort carbon starvation as well as low-storage maintenance respiration reductions. **(B)** Carbon Use Efficiency (CUE), or NPP/GPP. Decreases in carbon use efficiency imply relative increases in autotrophic respiration vs GPP. **(C)** Soil H_2O in the top 10 cm of soil. **(D)** β-Transpiration, soil moisture stress scalar affecting stomatal conductance. β-Transpiration reflects PFT response to soil matric potential (0–1 = low–high conductance).

scenarios in the 2090s, PP ecosystem GPP across management scenarios converged due to moisture limitation (**Supplementary Figure 12**). In conjunction, higher live PP biomass and R_a in MIROC AC1 and BAU scenarios led to lower NPP and CUE.

MC grid cells were the only PFT site-type on which moderately increased harvest (AC1) tree C stocks converged with BAU stocks by 2100 (**Supplementary Figure 14**). In both AC1 and AC2 scenarios, planting of the more drought and fire-tolerant PP PFT on warmer MC-sites led to increased GPP and R versus BAU. As a result, late-century NPP and NEP of both AC2 and AC1 scenarios faced low declines relative to BAU. Nonetheless, high AC2 harvest led to live and total site carbon that remained lower than BAU.

Discussion

Business-as-usual

Domain

By 2100, business-as-usual (BAU) live and dead forest carbon stocks in northern Idaho Rocky Mountain forests declined across RCP 8.5 climate scenarios and across plant functional types (PFT). However, declines in domain-scale forest carbon stocks of 22% (warmer, IPSL) and 6% (cooler, MIROC) did not result from an increase to average mortality rates through most of the period. Rather, we found that long-term stocks declines were characterized by declines in gross primary production (GPP) and net primary production (NPP) under contemporary levels of tree biomass and canopy area. Modeled forests experienced declining NPP and carbon use efficiency (CUE) that contributed to declining, negative net ecosystem carbon balance (NECB), and in turn the failure of forest canopy recovery following intermittent high fire and drought mortality years. Under increasing temperatures, NPP and NECB decline resulted from respiratory fluxes that were less sensitive to climate changes than primary production, consistent with previous research (Ciais et al., 2005; Schwalm et al., 2010). In the late 21st century, pronounced decreases to GPP resulted from increasing vapor pressure deficit (VPD), declining soil moisture, and decreasing stomatal conductance. 2090–2099 was the first decade in which drought-related forest mortality rates consistently increased across forest types and across climate model scenarios.

The forecasted declines of forest carbon stocks, crown area, and NECB in the region differed in timing and magnitude between climate scenarios under BAU management, indicating uncertainty as to whether forest carbon stock decline should be expected before the late 21st century (2080–2099). Annual precipitation increased under both climate scenarios, but was sufficient to prevent early to mid century NPP and NECB decline under moderate MIROC warming only. Further, 2025–2099 MIROC burned area was ∼40% of IPSL area due to non-linear impacts of fuel moisture on fire dynamics, causing average and maximum yearly MIROC tree fire mortality to be considerably lower. Despite the characteristic summer drought of much of the domain, these differing results indicate that the degree to which this relatively productive forest region of the WUSA will be increasingly vulnerable to direct negative impacts of warming though the mid-century (e.g., 1–3°C warming) is unclear, varying by climate scenario and also dependent on precipitation shifts. This result is consistent with recent modeling research with CLM 4.5, indicating higher relative fire and drought vulnerability in the southwest U.S. and Sierra Nevada than in the northern Rocky Mountains (Buotte et al., 2019). Previous LANDIS II simulations have also indicated delays in future C stock declines in the forests of the Northern Rocky Mountains (NRM) and Greater Yellowstone Ecosystem, in part due to increased precipitation (Henne et al., 2021; Walsh and Hudiburg, 2021). However, a NRM LANDIS II study also projected more distinct mid-century increases in burned area under RCP 8.5 (note: partially overlapping domain; Walsh and Hudiburg, 2021). This contrast highlights future vulnerability uncertainty arising from differing fire and vegetation dynamics across models as well as from differing climate model inputs and resolutions (Stenzel et al., 2019).

Plant functional type

Proportional decreases in year 2100 BAU tree C stocks, NPP, CUE, and crown cover were greatest for dry pine sites (PP and LP). While pine PFT traits (parameters. E.g., stomatal slope, root depth, bark depth, crown depth etc.) conferred relative drought and fire tolerance, tree carbon balance for shade-intolerant pine PFT-sites declined due to relatively high maintenance costs (e.g., respiration, leaf turnover). PP sites of this study represent the lower boundary of tree cover in the domain (Walsh and Hudiburg, 2021), generally occupying the hottest and driest forest land. Results support the notion that this drought-tolerant species (Martnez-Vilalta et al., 2004; Sala et al., 2005; Kwon et al., 2018) is nonetheless vulnerable to extended periods of drought and that negative drought impacts may be highest at hotter, lower elevation sites (Stevens-Rumann et al., 2017; Walsh and Hudiburg, 2021). Carbon starvation, rather

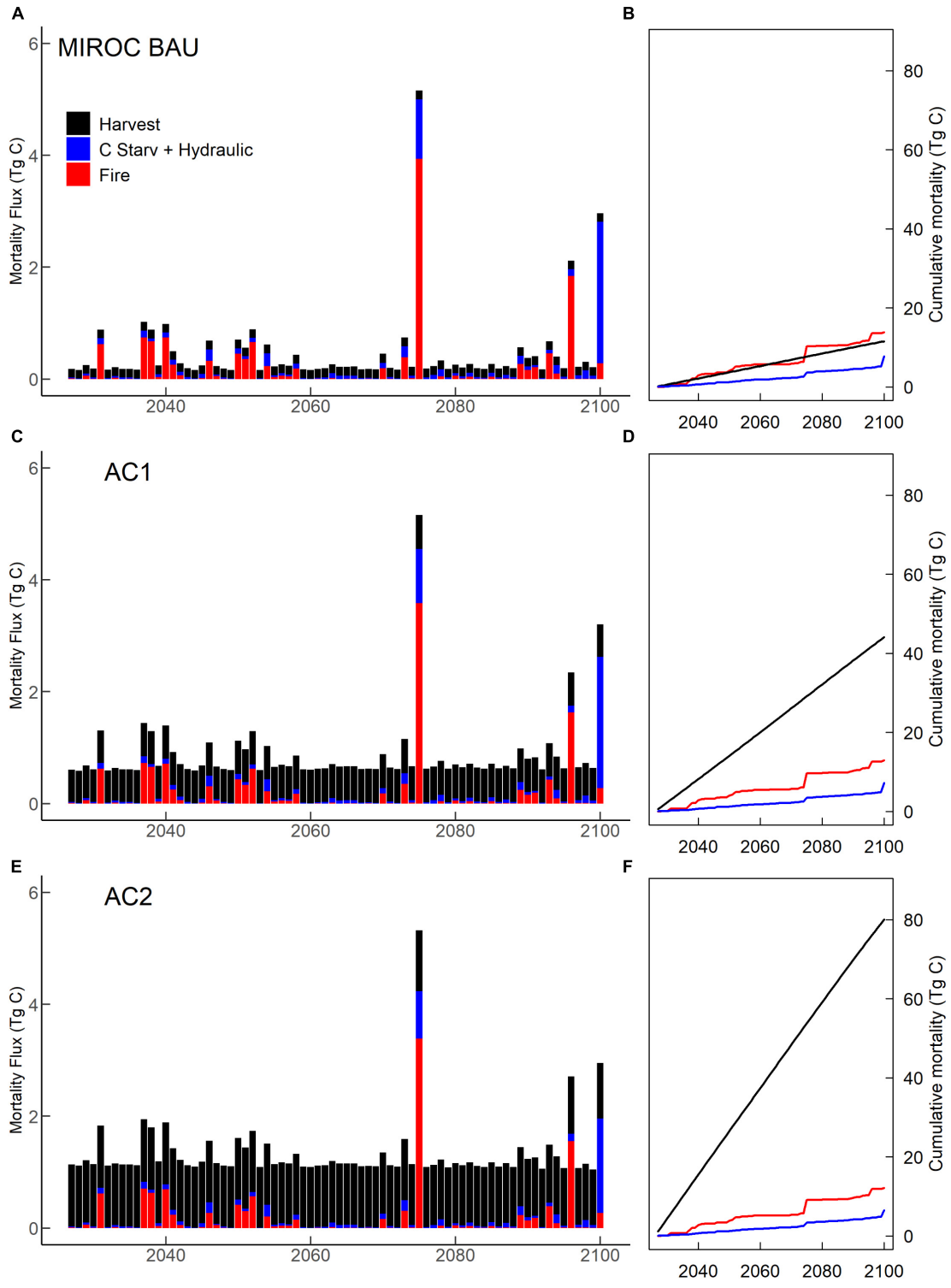

FIGURE 7
MIROC climate scenario tree mortality. **(A,C,E)** Annual mortality; and **(B,D,F)** cumulative mortality from wildfire, harvest, hydraulic failure and carbon starvation. **(A,B)** Business-as-usual (BAU). **(C,D)** Moderate harvest increase (AC1). **(E,F)** High harvest increase (AC2).

than hydraulic dysfunction, contributed to acute 2090s mortality of PP under IPSL climate (Sevanto et al., 2014). Higher typical moisture on MC and SF PFT-sites and lower maintenance costs delayed or prevented 21st century declines in PFT C stocks. Observed increases in burned area and mortality on DF, MC, and SF sites in the 2090s highlight an eventual projected reduction in fuel moisture limitations in moist, high biomass forests of the region (Arno, 1980; Arno et al., 2000). In contrast, the lack of modeled increase in PP and LP burned area resulted from lower fuel moisture, declining NPP, relatively low fire return intervals,

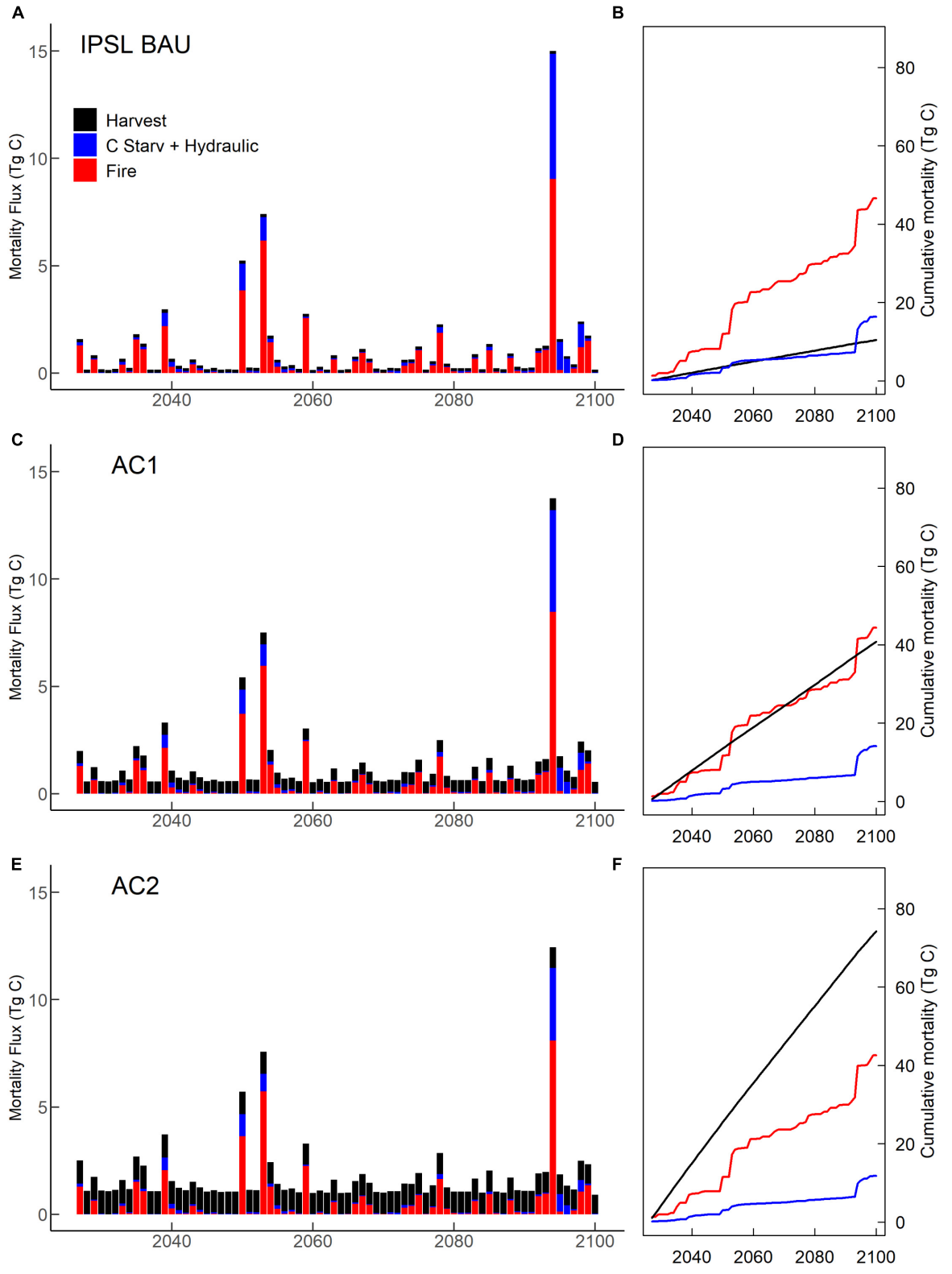

FIGURE 8
IPSL climate scenario tree mortality. **(A,C,E)** Annual mortality; and **(B,D,F)** cumulative mortality from wildfire, harvest, hydraulic failure and carbon starvation. **(A,B)** Business-as-usual (BAU). **(C,D)** Moderate harvest increase (AC1). **(E,F)** High harvest increase (AC2).

and declining fuel mass through the 21st century. End-of-century increases in drought related mortality for pine sites and burned area for moister mixed conifer and fir sites suggest that shifts in northern Idaho forest dynamics are primarily predicted in the long-term. However, we highlight that PFT distributions in this study are static across grid cells (i.e., fixed biogeography), leading to possible

10.3389/ffgc.2023.1146033

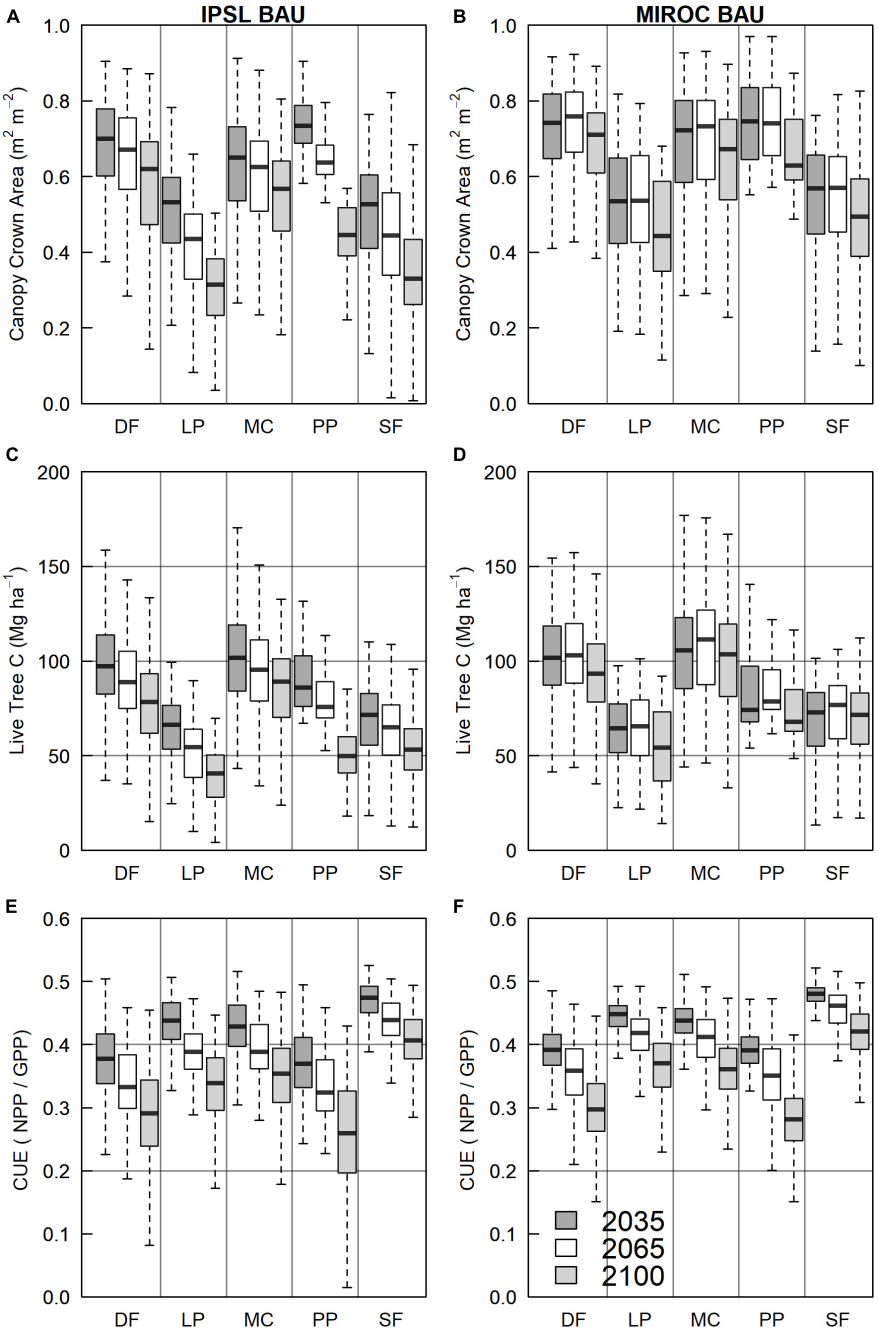

FIGURE 9
BAU forest structure and function by PFT site-type and climate scenario, 2025–2099. **(A,C,E)** IPSL climate; and **(B,D,F)** MIROC climate. **(A,B)** Canopy layer crown area. **(C,D)** Live tree carbon. **(E,F)** Carbon use efficiency (CUE). Boxes denote the interquartile range (IQ), horizontal bars show medians, and whiskers extend to extreme values within 1.5 times the IQ.

understatements of site resilience to stress via regional species diversity (DellaSala et al., 2013; Franklin and Johnson, 2013).

Increased harvest

We implemented moderate (AC1) and high (AC2) increased harvest scenarios to reflect large potential increases in timber harvest being considered on NRM USFS lands. In particular, the draft revision plan for the Nez Perce-Clearwater National Forest presents management alternatives that could implement multifold increases in regeneration harvest (i.e., even-aged harvest with post-harvest planting) (USDA, 2019). The high harvest scenario implemented in this study shifted future harvest levels near to 20th century maximums (USDA, 2022).

Across climate scenarios, both intensities of increased harvest resulted in domain carbon stock losses, forest cover losses, and increased total tree mortality relative to BAU through 2100. Consistent with previous research on the positive relationship between harvest intensity and ecosystem carbon

storage (Law et al., 2013, 2018; James et al., 2018), losses increased with harvest intensity. Higher increased harvest scenario mortality (by mass) occurred despite reductions in burned area and fire mortality, as lower fuel mass was achieved indirectly via impactful even-aged harvest. However, after 2060, reductions in residual forest stress under increased harvest also became evident, including reduced soil moisture limitation, increased stored carbon fraction, and increased CUE. Nonetheless, through approximately 2090, increased harvest scenario component carbon fluxes (GPP, NPP, R_a) remained lower than BAU scenarios due to reduced forest canopy area. After 2090, however, average GPP, NPP, and NECB of increased harvest scenarios exceeded BAU fluxes, while forest canopy cover converged with BAU at moderate harvest intensity (AC1). This pattern indicated that late 21st century climate stress began to lower the density of domain forest cover supported on the landscape, leading to greater impacts on higher biomass density BAU forests. Even so, total regional carbon stock deficits from increased harvest persisted through the entire simulation period. This suggests that increased even-aged harvest will not protect *in situ* stocks under near-term climate change and is consistent with previous research in the U.S. Pacific Northwest (Law et al., 2018, 2021).

The greatest benefit from increased harvest was experienced at the warmer and drier subset of mixed conifer PFT sites. There, moderate harvest increases (AC1) with planting of drought tolerant pine led to approximately equal tree biomass stocks and higher crown area in year 2100 than under BAU. Further, despite the higher maintenance costs of the ponderosa pine PFT (associated with parameters conferring relative shade-intolerance in FATES), deeper water access and more isohydric stomatal behavior (via stomatal slope) led to higher annual GPP, NPP, and CUE on such sites after 2090. However, convergence of mixed conifer site biomass levels across BAU and AC1 scenarios occurred late in the simulation period, leading to average increases in simulation period harvest C stock deficits versus BAU.

The management scenario results in this study demonstrate a tradeoff in which 21st century forest biomass and canopy area removal losses were incurred in return for a reduction in potential forest vulnerability in the 22nd century. Increased harvest and planting of fire and drought tolerant species increased NRM forest disturbance, mortality, and function loss through much of the 21st century, with little apparent reduction in vulnerability to natural stressors (fire, drought) in the short-term future. Only late-century increases in tree moisture stress fed back to lower growth, lower recruitment, and natural mortality rates in higher biomass-density BAU forests. Through 2100, however, all PFTs under all increased management scenarios demonstrated total live and dead biomass stocks that were lower than BAU stocks. The possible 22nd century convergence of management scenario biomass stocks and the likely positive impacts of planting drought and fire tolerant species on forest resilience are beyond the scope of this study. However, 21st century results indicate a need for further research into whether different management timing (e.g., later in the century) or methods could reduce late-century forest stress and decline while incurring lower time-averaged ecosystem carbon deficits (Hessburg et al., 2021; Prichard et al., 2021; Stenzel et al., 2021). Our management scenarios only implement the significant intensifications of regeneration harvest considered in draft NRM forest management plans (USDA, 2019). Changes to harvest levels in conjunction with prescribed fire, selective harvest, or other strategies are not modeled. This may in part explain the lack of near-term management benefits found in comparison to previous western U.S. modeling studies that implemented lower-mortality treatments such as selective harvest (Hurteau et al., 2016; Liang et al., 2018; McCauley et al., 2019).

Model discussion

Model advantages

A primary motivation for our use of CLM-FATES was its representation of distinct cohort crown areas within patches that can leave light gaps when individuals die. Patch post-disturbance recovery can then depend on the establishment and growth of new cohorts in available canopy space. Decreasing canopy area provides a spatial mechanism for forest function decline within grid cells (Fisher et al., 2015; Koven et al., 2019; FATES Development Team, 2022). These dynamics are not present in homogenous LAI models (i.e., non-spatial) like CLM 5.0 (Lawrence et al., 2018) or various successions extensions of LANDIS II (NECN, PnET; Scheller et al., 2011; De Bruijn et al., 2014), which represent vegetated column surfaces on which shrinking or expanding leaf biomass pools determine site leaf area index, rather than crown area. FATES representation of canopy space was essential to our results in U.S. Northern Rocky Mountain forests. Declining forest cover and biomass under climate change resulted from a combination of canopy mortality and gap generation; decreased carbon allocation to growth and seed production; and decreased tree recruitment and survival to maturity. Underlying the need for model functional gaps, the northern Idaho forest domain of this study has contemporary, observation-based tree canopy cover estimates of <60% (LANDFIRE Existing Vegetation Cover; DOI and USDA, 2022), with most of the remainder associated with post-forest disturbance canopy gaps. In this study, simulated primary production patterns emerged in large part from modeled gaps in forested canopy cover (60–65% in 2020, **Supplementary Figure 10**) that increased through 2100. While selective harvest was not explored as a forest treatment in this study, the gap dynamics of FATES would possibly refine previous thinning study results that represent modified forest stress via site LAI (Liang et al., 2018; Stenzel et al., 2021).

Model limitations

CLM-FATES lack of explicit cohort root area (vs depth) or root constraint within grid cell patches represents an important deficiency in this study's representation of forest response to soil moisture limitations under seasonal drought. As noted in the methods section, CLM-FATES does not represent separate soil water pools for FATES vegetated patches and instead aggregates soil water fluxes within grid cells. These dynamics can preclude water availability thresholds below which grid cells will no longer support a given PFT (i.e., fall outside PFT fundamental niche space). Grid cell canopy cover reductions instead lead to continual increases in per-tree soil water availability (negative feedback) and per-tree soil area can exceed feasible horizontal root spread. In this study, this dynamic was

potentially responsible for overestimated per-tree water availability, unconstrained negative feedbacks between tree density and stress, and forest resilience, rather than ecological tipping points, under warming climate.

Possible study overestimates of regional forest resilience to climate change stress may also have resulted from model seed distribution dynamics. FATES timestep seed production is aggregated across patches and then distributed in proportion to patch area. For this reason, FATES cannot represent limitations to disturbed patch seeding and regeneration that could realistically result from significant distances between live seed sources and disturbed areas. Within the NRM, observed forest gaps on the scale of hectares to square kilometers can persist for years to decades as a result of mass forest mortality from wildfire, bark beetles, and timber harvest (DOI and USDA, 2022).

Finally, forest plan revision documents for the domain's Idaho Panhandle and Nez Perce-Clearwater National Forests (USDA, 2015, 2019) also highlight observed and anticipated mortality resulting from biotic agents (insects and pathogens), particularly in productive, mid elevation, mixed conifer forests that include Douglas fir and grand fir. However, our study only represents the contribution of biotic agents to calibrated rates of recent species mortality (McNellis et al., 2021) via PFT-dependent background mortality rate parameters, and thus does not simulate prognostic changes to vulnerability to biotic-agent stress and mortality. Forest management revision plan alternatives that would cause species composition shifts (e.g., towards drought tolerant pine) at the scale of hundreds of thousands of acres per decade would create novel vegetation-stressor interactions and resulting species mortality rates would almost certainly shift (Das et al., 2016).

Conclusion

While much recent ecological research in western U.S. forest focuses on severe climate impacts such as increasing wildfire area (Westerling et al., 2006; Westerling, 2016; Abatzoglou et al., 2021), tree die-off (Anderegg et al., 2012; Allen et al., 2015), and cover conversions (Davis et al., 2019; Coop et al., 2020), it is also essential to highlight where and why lower vulnerability might occur. This is especially true in low vulnerability regions with high forest carbon density, where preservation priority is high (Law et al., 2018, 2021; Buotte et al., 2020). Based on our study's lack of intensifying forest vulnerability to drought and fire before 2050 and disagreement on post-mid-century decline across climate projections, we conclude that Idaho NRM forests represent one such moderate vulnerability region under BAU. This conclusion is supported by the low or moderate vulnerability to 21st century disturbance and carbon stock loss that has been reported in forest modeling studies in other subregions of the northwest U.S. (Henne et al., 2021; Walsh and Hudiburg, 2021), and contrasts with the greater vulnerability of drier or warmer portions of western U.S. forest (Buotte et al., 2019).

Uncertainties in global climate model projections are high at the end of the 21st century (IPCC, 2022). Further, climate model temperature-precipitation trends diverge from observations in the western U.S. (Abatzoglou et al., 2022), yet are essential to simulations of vegetation stress. In this study, climate uncertainty was reflected in divergent climate impacts to NRM forests. Highly variable scenario forest carbon stock decline timing and magnitude after 2050 resulted from the interaction of relatively high (IPSL) versus low (MIROC) RCP 8.5 warming with increases in annual precipitation. Because acute and consistent forest function loss was restricted to the late century, our confidence in increased 21st century NRM forest vulnerability is low.

The moderate vulnerability and high carbon density of modeled NRM forests indicates the persistent value of maintaining existing forest function through the 21st century (Buotte et al., 2020). In the context of low-certainty, long-term climate risks, conservative management strategies would seek to bolster forest resilience while minimizing landscape biomass and function losses to the extent possible. The 21st century increased harvest scenarios in this study instead implement a 'hard reset' approach that prescribes novel landscape compositions (USDA, 2019) and results in long-term forest cover and carbon stock losses. While the reduced forest cover density of increased harvest scenarios led to reduced moisture stress on a portion of the domain by 2100, high harvest mortality prevented ecosystem biomass stock parity with BAU.

This study represents the first regional application of CLM-FATES in the productive forests of the northwest U.S. and is an early application of the model towards applied research topics (Huang et al., 2020). With FATES coupling of CLM surface processes to heterogenous grid cell patches occupied by tree cohorts, we demonstrate 21st century climate and variable disturbance impacts that depend on declining forest cover in addition to declining biomass pool density (e.g., Walsh and Hudiburg, 2021). Our study implements a fixed PFT biogeography (i.e., PFT distribution across grid cells) and we highlight that limited spatiality to root water access (in contrast to spatial canopy light access) may limit the ability of the model to simulate competitive outcomes of variable PFT hydraulic strategies in moisture limited environments. Nonetheless, the capability of FATES to model shifting forest canopy area and the negative feedbacks between patch canopy density and tree stress were essential to projecting the mixed vulnerability of NRM forests to 21st century climate change.

Data availability statement

The data that support the findings of this study are openly available in the University of Idaho repository at https://doi.org/10.7923/2kee-sq55. Datasets include model inputs/outputs (FATES parameter set, domain, surfdat, land use, and history files). The FATES source code used in these experiments is available at: https://github.com/jestenzel/fates/releases/tag/nrockies_1.0.

Author contributions

JS, CK, and TH designed the study. JS implemented FATES code modifications and simulations. PB provided extensive model training and advice. All authors prepared the manuscript and approved the submitted version.

Funding

JS was supported by the National Science Foundation award number 1553049 and USDA NIFA award number 2022-67019-36435. CK was supported by the USDA NIFA award number 2022-67019-36435. TH was supported by the National Science Foundation award number 1553049. KB was supported by the National Institute of Food and Agriculture award number 2021-67034-34997.

Acknowledgments

We thank the two reviewers for valuable feedback that was essential for refining this work.

Conflict of interest

The authors declare that the research was conducted in the absence of any commercial or financial relationships that could be construed as a potential conflict of interest.

Publisher's note

All claims expressed in this article are solely those of the authors and do not necessarily represent those of their affiliated organizations, or those of the publisher, the editors and the reviewers. Any product that may be evaluated in this article, or claim that may be made by its manufacturer, is not guaranteed or endorsed by the publisher.

Supplementary material

The Supplementary Material for this article can be found online at: https://www.frontiersin.org/articles/10.3389/ffgc.2023.1146033/full#supplementary-material

References

Abatzoglou, J. T. (2013). Development of gridded surface meteorological data for ecological applications and modelling. *Int. J. Climatol.* 33, 121–131.

Abatzoglou, J. T., and Williams, A. P. (2016). Impact of anthropogenic climate change on wildfire across western US forests. *Proc. Natl. Acad. Sci. U.S.A.* 113, 11770–11775. doi: 10.1073/pnas.1607171113

Abatzoglou, J. T., Battisti, D. S., Williams, A. P., Hansen, W. D., Harvey, B. J., and Kolden, C. A. (2021). Projected increases in western US forest fire despite growing fuel constraints. *Commun. Earth Environ.* 2:227.

Abatzoglou, J. T., Marshall, A. M., Lute, A. C., and Safeeq, M. (2022). Precipitation dependence of temperature trends across the contiguous US. *Geophys. Res. Lett.* 49, 1–10. doi: 10.1007/s00704-022-04232-z

Allen, C. D., Breshears, D. D., and McDowell, N. G. (2015). On underestimation of global vulnerability to tree mortality and forest die-off from hotter drought in the Anthropocene. *Ecosphere* 6, 1–55.

Allen, C. D., Macalady, A. K., Chenchouni, H., Bachelet, D., McDowell, N., Vennetier, M., et al. (2010). A global overview of drought and heat-induced tree mortality reveals emerging climate change risks for forests. *For. Ecol. Manag.* 259, 660–684.

Anderegg, W. R., Berry, J. A., Smith, D. D., Sperry, J. S., Anderegg, L. D., and Field, C. B. (2012). The roles of hydraulic and carbon stress in a widespread climate-induced forest die-off. *Proc. Natl. Acad. Sci. U.S.A.* 109, 233–237.

Anderegg, W. R. L., Trugman, A. T., Wang, J., and Wu, C. (2022). Open science priorities for rigorous nature-based climate solutions. *PLoS Biol.* 20:e3001929. doi: 10.1371/journal.pbio.3001929

Anderson-Teixeira, K. J., Miller, A. D., Mohan, J. E., Hudiburg, T. W., Duval, B. D., and DeLucia, E. H. (2013). Altered dynamics of forest recovery under a changing climate. *Glob. Change Biol.* 19, 2001–2021. doi: 10.1111/gcb.12194

Arno, S. F. (1980). Forest fire history in the northern rockies. *J. For.* 78, 460–465.

Arno, S. F., Parsons, D. J., and Keane, R. E. (2000). Mixed-severity fire regimes in the northern rocky mountains: Consequences of fire exclusion and options for the future. *USDA For. Serv. Proc.* 5, 225–232.

Baker, K. V., Tai, X., Miller, M. L., and Johnson, D. M. (2019). Six co-occurring conifer species in northern idaho exhibit a continuum of hydraulic strategies during an extreme drought year. *AoB Plants* 11, 1–13. doi: 10.1093/aobpla/plz056

Bartowitz, K. J., Higuera, P. E., Shuman, B. N., McLauchlan, K. K., and Hudiburg, T. W. (2019). Post-fire carbon dynamics in subalpine forests of the Rocky Mountains. *Fire* 2:58.

Bartowitz, K. J., Walsh, E. S., Stenzel, J. E., Kolden, C. A., and Hudiburg, T. W. (2022). Forest carbon emission sources are not equal: Putting fire, harvest, and fossil fuel emissions in context. *Front. For. Glob. Change* 5:867112. doi: 10.3389/ffgc.2022.867112

Berner, L. T., Law, B. E., Meddens, A. J. H., and Hicke, J. A. (2017). Tree mortality from fires, bark beetles, and timber harvest during a hot and dry decade in the western United States (2003–2012). *Environ. Res. Lett.* 12:65005.

Bollenbacher, B. L., Graham, R. T., and Reynolds, K. M. (2014). Regional forest landscape restoration priorities: Integrating historical conditions and an uncertain future in the northern rocky mountains. *J. For.* 112, 474–483.

Bonan, G. (2019). *Climate change and terrestrial ecosystem modeling*. Cambridge: Cambridge University Press.

Bonan, G. B. (2008). Forests and climate change: Forcings, feedbacks, and the climate benefits of forests. *Science* 320, 1444–1449.

Brown, R. T., Agee, J. K., and Franklin, J. F. (2004). Forest restoration and fire: Principles in the context of place. *Conserv. Biol.* 18, 903–912.

Buotte, P. C., Koven, C. D., Xu, C., Shuman, J. K., Goulden, M. L., Levis, S., et al. (2021). Capturing functional strategies and compositional dynamics in vegetation demographic models. *Biogeosciences* 18, 4473–4490. doi: 10.1186/1475-2875-9-228

Buotte, P. C., Law, B. E., Ripple, W. J., and Berner, L. T. (2020). Carbon sequestration and biodiversity co-benefits of preserving forests in the western United States. *Ecol. Appl.* 30, 1–11. doi: 10.1002/eap.2039

Buotte, P. C., Levis, S., Law, B. E., Hudiburg, T. W., Rupp, D. E., and Kent, J. J. (2019). Near-future forest vulnerability to drought and fire varies across the western United States. *Glob. Change Biol.* 25, 290–303. doi: 10.1111/gcb.14490

Case, M. J., Johnson, B. G., Bartowitz, K. J., and Hudiburg, T. W. (2021). Forests of the future: Climate change impacts and implications for carbon storage in the Pacific Northwest, USA. *For. Ecol. Manag.* 482:118886.

Chapin, F. S., Woodwell, G. M., Randerson, J. T., Rastetter, E. B., Lovett, G. M., Baldocchi, D. D., et al. (2006). Reconciling carbon-cycle concepts, terminology, and methods. *Ecosystems* 9, 1041–1050.

Ciais, P., Reichstein, M., Viovy, N., Granier, A., Ogée, J., Allard, V., et al. (2005). Europe-wide reduction in primary productivity caused by the heat and drought in 2003. *Nature* 437, 529–533. doi: 10.1038/nature03972

Coop, J. D., Parks, S. A., Stevens-Rumann, C. S., Crausbay, S. D., Higuera, P. E., Hurteau, M. D., et al. (2020). Wildfire-driven forest conversion in western North American landscapes. *BioScience* 70, 659–673. doi: 10.1093/biosci/biaa061

Das, A. J., Stephenson, N. L., and Davis, K. P. (2016). Why do trees die? Characterizing the drivers of background tree mortality. *Ecology* 97, 2616–2627. doi: 10.1002/ecy.1497

Davis, K. T., Dobrowski, S. Z., Higuera, P. E., Holden, Z. A., Veblen, T. T., Rother, M. T., et al. (2019). Wildfires and climate change push low-elevation forests across

a critical climate threshold for tree regeneration. *Proc. Natl. Acad. Sci. U.S.A.* 116, 6193–6198. doi: 10.1073/pnas.1815107116

De Bruijn, A. M., Gustafson, E. J., Sturtevant, B. R., Foster, J. R., Miranda, B. R., Lichti, N. I., et al. (2014). Toward more robust projections of forest landscape dynamics under novel environmental conditions: Embedding PnET within LANDIS-II. *Ecol. Model.* 287, 44–57.

DellaSala, D. A., Anthony, R. G., Bond, M. L., Fernandez, E. S., Frissell, C. A., Hanson, C. T., et al. (2013). Alternative views of a restoration framework for federal forests in the Pacific Northwest. *J. For.* 111, 420–429.

DeLucia, E. H., Drake, J. E., Thomas, R. B., and Gonzalez-Meler, M. (2007). Forest carbon use efficiency: Is respiration a constant fraction of gross primary production?. *Glob. Change Biol.* 13, 1157–1167. doi: 10.1093/treephys/tpz034

DOI and USDA (2022). *LANDFIRE: LANDFIRE existing vegetation type layer. Online*. Available online at: https://www.landfire.gov/evc.php (accessed October 16, 2022).

Edburg, S. L., Hicke, J. A., Lawrence, D. M., and Thornton, P. E. (2011). Simulating coupled carbon and nitrogen dynamics following mountain pine beetle outbreaks in the Western United States. *J. Geophys. Res. Biogeosci.* 116, 1–15.

Eidenshink, J., Schwind, B., Brewer, K., Zhu, Z.-L., Quayle, B., and Howard, S. (2007). A project for monitoring trends in burn severity. *Fire Ecol.* 3, 3–21.

Evangelista, P. H., Kumar, S., Stohlgren, T. J., and Young, N. E. (2011). Assessing forest vulnerability and the potential distribution of pine beetles under current and future climate scenarios in the interior west of the US. *For. Ecol. Manag.* 262, 307–316.

Evans, M. E. K., Merow, C., Record, S., McMahon, S. M., and Enquist, B. J. (2016). Towards process-based range modeling of many species. *Trends Ecol. Evol.* 31, 860–871.

FATES Development Team (2022). *FATES documentation. Release d2*, eds R. A. Fisher, R. G. Knox, C. D. Koven, G. Lemieux, C. Xu, B. Christofferson, et al. Available online at: https://fates-users-guide.readthedocs.io/_/downloads/tech-doc/en/stable/pdf/

Finco, M., Quayle, B., Zhang, Y., Lecker, J., Megown, K. A., and Brewer, C. K. (2012). "Monitoring trends and burn severity (MTBS): Monitoring wildfire activity for the past quarter century using LANDSAT data," in *Proceedings: Moving from status to trends: Forest inventory and analysis (FIA) symposium; 2012 December 4-6; Baltimore, MD*, eds R. Morin and G. Liknes (Newtown Square, PA: U.S. Department of Agriculture, Forest Service, Northern Research Station), 222–228.

Fisher, R. A., and Koven, C. D. (2020). Perspectives on the future of land surface models and the challenges of representing complex terrestrial systems. *J. Adv. Model. Earth Syst.* 12:e2018MS001453.

Fisher, R. A., Koven, C. D., Anderegg, W. R. L., Christoffersen, B. O., Dietze, M. C., Farrior, C. E., et al. (2018). Vegetation demographics in earth system models: A review of progress and priorities. *Glob. Change Biol.* 24, 35–54. doi: 10.1111/gcb.13910

Fisher, R. A., Muszala, S., Verteinstein, M., Lawrence, P., Xu, C., McDowell, N. G., et al. (2015). Taking off the training wheels: The properties of a dynamic vegetation model without climate envelopes, CLM4.5(ED). *Geosci. Model Dev.* 8, 3593–3619.

Franklin, J. F., and Johnson, K. N. (2013). A restoration framework for federal forests in the Pacific Northwest. *J. For.* 110, 429–439.

Gibson, C. E., and Morgan, P. (2005). *Fire history polygons for northern rockies: 1889–2003. Vector digital data*. Moscow, ID: University of Idaho.

Gray, A., Brandeis, T., Shaw, J., McWilliams, W., and Miles, P. (2012). Forest inventory and analysis database of the United States of America (FIA). *Biodivers. Ecol.* 4, 225–231.

Gruell, G. E. (1982). *Seventy years of vegetative change in a managed ponderosa pine forest in Western Montana–implications for resource management*, Vol. 130. Ogden, UT: US Department of Agriculture, Forest Service, Intermountain Forest and Range.

Gruell, G. E. (1983). *Fire and vegetative trends in the northern rockies: Interpretations from 1871-1982 Photographs. General technical report*. Washington, DC: US Department of Agriculture, Forest Service (INT-158).

Hanbury-Brown, A. R., Ward, R. E., and Kueppers, L. M. (2022). Forest regeneration within earth system models: Current process representations and ways forward. *New Phytol.* 235, 20–40. doi: 10.1111/nph.18131

Henne, P. D., Hawbaker, T. J., Scheller, R. M., Zhao, F., He, H. S., Xu, W., et al. (2021). Increased burning in a warming climate reduces carbon uptake in the greater yellowstone ecosystem despite productivity gains. *J. Ecol.* 109, 1148–1169.

Hessburg, P. F., Prichard, S. J., Hagmann, R. K., Povak, N. A., and Lake, F. K. (2021). Wildfire and climate change adaptation of western North American forests: A case for intentional management. *Ecol. Appl.* 31:e02432.

Higuera, P. E., and Abatzoglou, J. T. (2021). Record-setting climate enabled the extraordinary 2020 fire season in the Western United States. *Glob. Change Biol.* 27, 1–2. doi: 10.1111/gcb.15388

Huang, M., Xu, Y., Longo, M., Keller, M., Knox, R. G., Koven, C. D., et al. (2020). Assessing impacts of selective logging on water, energy, and carbon budgets and ecosystem dynamics in amazon forests using the functionally assembled terrestrial ecosystem simulator. *Biogeosciences* 17, 4999–5023.

Hudiburg, T. W., Higuera, P. E., and Hicke, J. A. (2017). Fire-regime variability impacts forest carbon dynamics for centuries to Millennia. *Biogeosciences* 14, 3873–3882.

Hudiburg, T. W., Law, B. E., and Thornton, P. E. (2013). Evaluation and improvement of the community land model (CLM4) in oregon forests. *Biogeosciences* 10, 453–470.

Hudiburg, T. W., Law, B. E., Moomaw, W. R., Harmon, M. E., and Stenzel, J. E. (2019). Meeting GHG reduction targets requires accounting for all forest sector emissions. *Environ. Res. Lett.* 14:095005.

Hudiburg, T., Law, B., Turner, D. P., Campbell, J., Donato, D., and Duane, M. (2009). Carbon dynamics of oregon and Northern California forests and potential land-based carbon storage. *Ecol. Appl.* 19, 163–180. doi: 10.1890/07-2006.1

Hurteau, M. D., Liang, S., Martin, K. L., North, M. P., Koch, G. W., and Hungate, B. A. (2016). Restoring forest structure and process stabilizes forest carbon in wildfire-prone southwestern ponderosa pine forests. *Ecol. Appl.* 26, 382–391. doi: 10.1890/15-0337

Hurtt, G. C., Chini, L., Sahajpal, R., Frolking, S., Bodirsky, B. L., Calvin, K., et al. (2020). Harmonization of global land-use change and management for the period 850-2100 (LUH2 for CMIP6. *Geosci. Model Dev. Discuss.* 13, 5425–5464.

IPCC (2022). "Climate change 2022: Impacts, adaptation, and vulnerability," in *Contribution of working group II to the sixth assessment report of the intergovernmental panel on climate change*, eds B. R. H.-O. Pörtner, D. C. Roberts, M. Tignor, E. S. Poloczanska, K. Mintenbeck, A. Alegría, et al. (Cambridge: Cambridge University Press).

Irvine, J., Law, B. E., Kurpius, M. R., Anthoni, P. M., Moore, D., and Schwarz, P. A. (2004). Age-related changes in ecosystem structure and function and effects on water and carbon exchange in ponderosa pine. *Tree Physiol.* 24, 753–763. doi: 10.1093/treephys/24.7.753

Irvine, J., Law, B. E., Martin, J. G., and Vickers, D. (2008). Interannual variation in Soil CO2 efflux and the response of root respiration to climate and canopy gas exchange in mature ponderosa pine. *Glob. Change Biol.* 14, 2848–2859.

James, J. N., Kates, N., Kuhn, C. D., Littlefield, C. E., Miller, C. W., Bakker, J. D., et al. (2018). The effects of forest restoration on ecosystem carbon in western North America: A systematic review. *For. Ecol. Manag.* 429, 625–641.

Kattge, J., Bönisch, G., Díaz, S., Lavorel, S. I, Prentice, C., Leadley, P., et al. (2020). TRY plant trait database – enhanced coverage and open access. *Glob. Change Biol.* 26, 119–188. doi: 10.1111/gcb.14904

Koch, E. (1942). *History of the 1910 forest fires in Idaho and Western Montana*. Moscow: University of Idaho Library.

Koch, E. (1978). *When the mountrains roared: Stories of the 1910 fire*. Washington, DC: US Department of Agriculture, Forest Service.

Kolden, C. A., Smith, A. M. S., and Abatzoglou, J. T. (2015). Limitations and utilisation of monitoring trends in burn severity products for assessing wildfire severity in the USA. *Int. J. Wildland Fire* 24, 1023–1028.

Körner, C., Asshoff, R., Bignucolo, O., Hättenschwiler, S., Keel, S. G., Peláez-Riedl, S., et al. (2005). Ecology: Carbon flux and growth in mature deciduous forest trees exposed to elevated CO2. *Science* 309, 1360–1362. doi: 10.1126/science.1113977

Koven, C., Knox, R., Fisher, R., Chambers, J., Christoffersen, B., Davies, S., et al. (2019). Benchmarking and parameter sensitivity of physiological and vegetation dynamics using the functionally assembled terrestrial ecosystem simulator (FATES) at Barro Colorado Island, Panama. *Biogeosci. Discuss.* 17, 3017–3044.

Kwon, H., Law, B. E., Thomas, C. K., and Johnson, B. G. (2018). The influence of hydrological variability on inherent water use efficiency in forests of contrasting composition, age, and precipitation regimes in the Pacific Northwest. *Agric. For. Meteorol.* 249, 488–500.

Lambert, M. S. A., Tang, H., Aas, K. S., Stordal, F., Fisher, R. A., Fang, Y., et al. (2022). Inclusion of a cold hardening scheme to represent frost tolerance is essential to model realistic plant hydraulics in the Arctic – Boreal Zone in CLM5 . 0-FATES-Hydro. *Geosci. Model Dev. Discuss.* [preprint]. doi: 10.5194/gmd-2022-136

Law, B. E., and Berner, L. T. (2015). *NACP TERRA-PNW: Forest plant traits, NPP, biomass, and soil properties, 1999-2014*. Oak Ridge, TN: ORNL DAAC.

Law, B. E., Berner, L. T., Buotte, P. C., Mildrexler, D. J., and Ripple, W. J. (2021). Strategic forest reserves can protect biodiversity in the Western United States and mitigate climate change. *Commun. Earth Environ.* 2, 1–13.

Law, B. E., Hudiburg, T. W., and Luyssaert, S. (2013). Thinning effects on forest productivity: Consequences of preserving old forests and mitigating impacts of fire and drought. *Plant Ecol. Divers.* 6, 73–85.

Law, B. E., Hudiburg, T. W., Berner, L. T., Kent, J. J., Buotte, P. C., and Harmon, M. E. (2018). Land use strategies to mitigate climate change in carbon dense temperate forests. *Proc. Natl. Acad. Sci. U.S.A.* 115, 3663–3668. doi: 10.1073/pnas.1720064115

Law, B. E., Moomaw, W. R., Hudiburg, T. W., Schlesinger, W. H., Sterman, J. D., and Woodwell, G. M. (2022). Creating strategic reserves to protect forest carbon and reduce biodiversity losses in the United States. *Land* 11, 1–15.

Law, B. E., Thornton, P. E., Irvine, J., Anthoni, P. M., and Van Tuyl, S. (2001a). Carbon storage and fluxes in ponderosa pine forests at different developmental stages. *Glob. Change Biol.* 7, 755–777.

Law, B. E., Van Tuyl, S., Cescatti, A., and Baldocchi, D. D. (2001b). Estimation of leaf area index in open-canopy ponderosa pine forests at different successional stages and management regimes in oregon. *Agric. For. Meteorol.* 108, 1–14.

Law, B., Sun, O. J., Campbell, J., Van Tuyl, S., and Thornton, P. (2003). Changes in carbon storage and fluxes in a chronoseuence of ponderosa pine. *Glob. Change Biol.* 4, 510–524.

Lawrence, D. M., Fisher, R. A., Koven, C. D., Oleson, K. W., Swenson, S. C., Bonan, G., et al. (2019). The community land model version 5: Description of new features, benchmarking, and impact of forcing uncertainty. *J. Adv. Model. Earth Syst.* 11, 4245–4287.

Lawrence, D., Fisher, R., Koven, C., Oleson, K., Swenson, S., and Vertenstein, M. (2018). *Technical description of version 5.0 of the community land model (CLM)*. Boulder, CO: National Center for Atmospheric Research.

Liang, S., Hurteau, M. D., and Westerling, A. L. (2018). Large-scale restoration increases carbon stability under projected climate and wildfire regimes. *Front. Ecol. Environ.* 16:207–212. doi: 10.1002/fee.1791

Lutz, J. A., Larson, A. J., Swanson, M. E., and Freund, J. A. (2012). Ecological importance of large-diameter trees in a temperate mixed-conifer forest. *PLoS One* 7:e36131. doi: 10.1371/journal.pone.0036131

Martnez-Vilalta, J., Sala, A., and Piol, J. (2004). The hydraulic architecture of pinaceae–a review. *Plant Ecol.* 171, 3–13.

McCauley, L. A., Robles, M. D., Woolley, T., Marshall, R. M., Kretchun, A., and Gori, D. F. (2019). Large-scale forest restoration stabilizes carbon under climate change in Southwest United States. *Ecol. Appl.* 29:e01979. doi: 10.1002/eap.1979

McNellis, B. E., Smith, A. M. S., Hudak, A. T., and Strand, E. K. (2021). Tree mortality in Western U.S. Forests forecasted using forest inventory and random forest classification. *Ecosphere* 12:e03419.

Morgan, P., Heyerdahl, E. K., and Gibson, C. E. (2008). Multi-season climate synchronized forest fires throughout the 20th century, Northern Rockies, USA. *Ecology* 89, 717–728. doi: 10.1890/06-2049.1

Muthukrishnan, R., Hayes, K., Bartowitz, K., Cattau, M. E., Harvey, B. J., Lin, Y., et al. (2022). Harnessing NEON to evaluate ecological tipping points: Opportunities, challenges, and approaches. *Ecosphere* 13, 1–16.

Naficy, C., Sala, A., Keeling, E. G., Graham, J., and DeLuca, T. H. (2010). Interactive effects of historical logging and fire exclusion on ponderosa pine forest structure in the Northern Rockies. *Ecol. Appl.* 20, 1851–1864. doi: 10.1890/09-0217.1

Nagy, R. C., Balch, J. K., Bissell, E. K., Cattau, M. E., Glenn, N. F., Halpern, B. S., et al. (2021). Harnessing the NEON data revolution to advance open environmental science with a diverse and data-capable community. *Ecosphere* 12:e03833.

Omernik, J. M., and Griffith, G. E. (2014). Ecoregions of the conterminous united states: Evolution of a hierarchical spatial framework. *Environ. Manag.* 54, 1249–1266. doi: 10.1007/s00267-014-0364-1

Parks, S. A., and Abatzoglou, J. T. (2020). Warmer and drier fire seasons contribute to increases in area burned at high severity in Western US forests from 1985 to 2017. *Geophys. Res. Lett.* 47, 1–10.

Peters, G. P., Andrew, R. M., Boden, T., Canadell, J. G., Ciais, P., Le Quéré, C., et al. (2013). The challenge to keep global warming below 2C. *Nat. Clim. Change* 3, 4–6. doi: 10.3390/nano13142050

Picotte, J. J., Bhattarai, K., Howard, D., Lecker, J., Epting, J., Quayle, B., et al. (2020). Changes to the monitoring trends in burn severity program mapping production procedures and data products. *Fire Ecol.* 16:16.

Prichard, S. J., Hessburg, P. F., Hagmann, R. K., Povak, N. A., Dobrowski, S. Z., Hurteau, M. D., et al. (2021). Adapting Western North American forests to climate change and wildfires: Ten common questions. *Ecol. Appl.* 31:E02433. doi: 10.1002/eap.2433

Ramsfield, T. D., Bentz, B. J., Faccoli, M., Jactel, H., and Brockerhoff, E. G. (2016). Forest health in a changing world: Effects of globalization and climate change on forest insect and pathogen impacts. *Forestry* 89, 245–252.

Ruefenacht, B., Finco, M. V., Czaplewski, R., Helmer, E., Blackard, J., Holden, G. R., et al. (2008). Mapping using forest inventory and analysis data. *Photogramm. Eng. Remote Sensing* 74, 1379–1388.

Running, S., and Zhao, M. (2021). MODIS/Terra net primary production gap-filled yearly L4 Global 500m SIN grid V061 [Dataset]. NASA EOSDIS land processes DAAC. Available online at: https://doi.org/10.5067/MODIS/MOD17A3HGF.061 (accessed October 1, 2022).

Rupp, D. E., Abatzoglou, J. T., and Mote, P. W. (2017). Projections of 21st century climate of the columbia river basin. *Clim. Dyn.* 49, 1783–1799.

Sala, A., Peters, G. D., McIntyre, L. R., and Harrington, M. G. (2005). Physiological responses of ponderosa pine in western montana to thinning, prescribed fire and burning season. *Tree Physiol.* 25, 339–348.

Scheiter, S., Langan, L., and Higgins, S. I. (2013). Next-generation dynamic global vegetation models: Learning from community ecology. *New Phytol.* 198, 957–969. doi: 10.1111/nph.12210

Scheller, R. M., Hua, D., Bolstad, P. V., Birdsey, R. A., and Mladenoff, D. J. (2011). The effects of forest harvest intensity in combination with wind disturbance on carbon dynamics in lake states mesic forests. *Ecol. Model.* 222, 144–153.

Schimel, D., Kittel, T. G. F., Running, S., Monson, R., Turnipseed, A., and Anderson, D. (2002). Carbon sequestration studied in Western U.S. mountains. *Eos* 83, 445–449.

Schwalm, C. R., Williams, C. A., Schaefer, K., Arneth, A., Bonal, D., Buchmann, N., et al. (2010). Assimilation exceeds respiration sensitivity to drought: A FLUXNET synthesis. *Glob. Change Biol.* 16, 657–670.

Schwalm, C. R., Williams, C. A., Schaefer, K., Baldocchi, D., Black, T. A., Goldstein, A. H., et al. (2012). Reduction in carbon uptake during turn of the century drought in Western North America. *Nat. Geosci.* 5, 551–556.

Scott, L. M., and Janikas, M. V. (2009). "Spatial statistics in ArcGIS," in *Handbook of applied spatial analysis: Software tools, methods and applications* (Heidelberg: Springer Berlin Heidelberg), 27–41.

Sevanto, S., Mcdowell, N. G., Dickman, L. T., Pangle, R., and Pockman, W. T. (2014). How do trees die? A test of the hydraulic failure and carbon starvation hypotheses. *Plant Cell Environ.* 37, 153–161. doi: 10.1111/pce.12141

Smith, H. Y., and Arno, S. F. (1999). *Eighty-eight years of change in a managed ponderosa pine forest*. Ogden, UT: US Department Agriculture, Forest Service, Rocky Mountain Research Station.

Smith, J. E., Domke, G. M., Nichols, M. C., and Walters, B. F. (2019). Carbon stocks and stock change on federal forest lands of the United States. *Ecosphere* 10:e02637. doi: 10.1073/pnas.1512542112

Stenzel, J. E., Bartowitz, K. J., Hartman, M. D., Lutz, J. A., Kolden, C. A., Smith, A. M. S., et al. (2019). Fixing a snag in carbon emissions estimates from wildfires. *Glob. Change Biol.* 25, 3985–3994. doi: 10.1111/gcb.14716

Stenzel, J. E., Berardi, D. M., Walsh, E. S., and Hudiburg, T. W. (2021). Restoration thinning in a drought-prone idaho forest creates a persistent carbon deficit. *J. Geophys. Res. Biogeosci.* 126, 1–18.

Stevens-Rumann, C. S., Kemp, K. B., Higuera, P. E., Harvey, B. J., Rother, M. T., Donato, D. C., et al. (2017). Evidence for declining forest resilience to wildfires under climate change. *Ecol. Lett.* 21, 243–252.

Sun, O. J., Campbell, J., Law, B. E., and Wolf, V. (2004). Dynamics of carbon stocks in soils and detritus across chronosequences of different forest types in the Pacific Northwest, USA. *Glob. Change Biol.* 10, 1470–1481.

Thonicke, K., Spessa, A., Prentice, I. C., Harrison, S. P., Dong, L., and Carmona-Moreno, C. (2010). The influence of vegetation, fire spread and fire behaviour on biomass burning and trace gas emissions: Results from a process-based model. *Biogeosciences* 7, 1991–2011.

Thurner, M., Beer, C., Santoro, M., Carvalhais, N., Wutzler, T., Schepaschenko, D., et al. (2014). Carbon stock and density of northern boreal and temperate forests. *Glob. Ecol. Biogeogr.* 23, 297–310. doi: 10.1002/eap.1749

Turner, M. G., Braziunas, K. H., Hansen, W. D., and Harvey, B. J. (2019). Short-interval severe fire erodes the resilience of subalpine lodgepole pine forests. *Proc. Natl. Acad. Sci. U.S.A.* 166, 11319–11328. doi: 10.1073/pnas.1902841116

USDA (2015). *Idaho panhandle national forests land management plan, 2015 Revision*. Washington, DC: USDA.

USDA (2019). *Draft land management plan for the nez perce-clearwater national forests*. Washington, DC: USDA.

USDA (2022). *Forest service activity tracking system*. Washington, DC: USDA.

VanderWeide, B. L., and Hartnett, D. C. (2011). Fire resistance of tree species explains historical gallery forest community composition. *For. Ecol. Manag.* 261, 1530–1538.

Walsh, E. S., and Hudiburg, T. W. (2019). An integration framework for linking avifauna niche and forest landscape models. *PLoS One* 14:e0217299. doi: 10.1371/journal.pone.0217299

Walsh, E. S., and Hudiburg, T. W. (2021). Response of avian cavity nesters and carbon dynamics to forest management and climate change in the Northern Rockies. *Ecosphere* 12:e03636.

Westerling, A. L. (2016). Increasing western US forest wildfire activity: Sensitivity to changes in the timing of spring. *Philos. Trans. R. Soc. B Biol. Sci.* 371:20150178.

Westerling, A. L., Hidalgo, H. G., Cayan, D. R., and Swetnam, T. W. (2006). Warming and earlier spring increase western U.S. forest wildfire activity. *Science* 313, 940–943.

Zhao, M., and Running, S. W. (2010). Drought-induced reduction in global. *Science* 329, 940–943.